

Hydrothermal $^{15}\text{N}/^{14}\text{N}$ abundances constrain the origins of mantle nitrogen


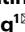
<https://doi.org/10.1038/s41586-020-2173-4>

Received: 4 July 2019

Accepted: 4 February 2020

Published online: 15 April 2020

 Check for updates

J. Labidi^{1,11}, P. H. Barry², D. V. Bekaert³, M. W. Broadley³, B. Marty³, T. Giunta⁴, O. Warr⁴, B. Sherwood Lollar⁴, T. P. Fischer⁵, G. Avice⁶, A. Caracausi⁷, C. J. Ballentine⁸, S. A. Halldórsson⁹, A. Stefánsson⁹, M. D. Kurz², I. E. Kohl¹⁰ & E. D. Young¹¹

Nitrogen is the main constituent of the Earth's atmosphere, but its provenance in the Earth's mantle remains uncertain. The relative contribution of primordial nitrogen inherited during the Earth's accretion versus that subducted from the Earth's surface is unclear^{1–6}. Here we show that the mantle may have retained remnants of such primordial nitrogen. We use the rare $^{15}\text{N}/^{14}\text{N}$ isotopologue of N_2 as a new tracer of air contamination in volcanic gas effusions. By constraining air contamination in gases from Iceland, Eifel (Germany) and Yellowstone (USA), we derive estimates of mantle $\delta^{15}\text{N}$ (the fractional difference in $^{15}\text{N}/^{14}\text{N}$ from air), $\text{N}_2/^{36}\text{Ar}$ and $\text{N}_2/^{3}\text{He}$. Our results show that negative $\delta^{15}\text{N}$ values observed in gases, previously regarded as indicating a mantle origin for nitrogen^{7–10}, in fact represent dominantly air-derived N_2 that experienced $^{15}\text{N}/^{14}\text{N}$ fractionation in hydrothermal systems. Using two-component mixing models to correct for this effect, the $^{15}\text{N}/^{14}\text{N}$ data allow extrapolations that characterize mantle endmember $\delta^{15}\text{N}$, $\text{N}_2/^{36}\text{Ar}$ and $\text{N}_2/^{3}\text{He}$ values. We show that the Eifel region has slightly increased $\delta^{15}\text{N}$ and $\text{N}_2/^{36}\text{Ar}$ values relative to estimates for the convective mantle provided by mid-ocean-ridge basalts¹¹, consistent with subducted nitrogen being added to the mantle source. In contrast, we find that whereas the Yellowstone plume has $\delta^{15}\text{N}$ values substantially greater than that of the convective mantle, resembling surface components^{12–15}, its $\text{N}_2/^{36}\text{Ar}$ and $\text{N}_2/^{3}\text{He}$ ratios are indistinguishable from those of the convective mantle. This observation raises the possibility that the plume hosts a primordial component. We provide a test of the subduction hypothesis with a two-box model, describing the evolution of mantle and surface nitrogen through geological time. We show that the effect of subduction on the deep nitrogen cycle may be less important than has been suggested by previous investigations. We propose instead that high mid-ocean-ridge basalt and plume $\delta^{15}\text{N}$ values may both be dominantly primordial features.

Differentiated bodies from our Solar System have rocky mantles with $^{15}\text{N}/^{14}\text{N}$ ratios within $\pm 15\%$ of modern terrestrial air^{16,17}. This is true for Earth's convective mantle, which has a $\delta^{15}\text{N}$ value of approximately $-5 \pm 3\%$, based on measurements from diamonds^{5,18} and basalts that have been filtered for air contamination^{3,11}. Conversely, volatile-rich chondritic meteorites exhibit highly variable $\delta^{15}\text{N}$ values between $-20 \pm 11\%$ for enstatite chondrites and $48 \pm 9\%$ for CI carbonaceous chondrites^{16,19}. The distinct $^{15}\text{N}/^{14}\text{N}$ of rocky mantles relative to the chondrites may reflect inheritance of N from a heterogeneous mixture of chondritic precursors³. Alternatively, the relatively high $^{15}\text{N}/^{14}\text{N}$ values could be the result of evaporative losses²⁰, or equilibrium partitioning of N isotopes between metal cores and rocky mantles^{21,22}.

For Earth, plate tectonics allows for another interpretation¹. Geochemists have suggested that mantle $\delta^{15}\text{N}$ values reflect subduction of nitrogen from the surface. Some of the evidence comes from studies of gases from mantle plumes. On Earth, mantle plumes with high $^3\text{He}/^4\text{He}$ ratios relative to mid-ocean-ridge basalts (MORBs) result from melting of relatively undegassed portions of the deep mantle²³. Nitrogen data are sparse, but plumes with both high and low $^3\text{He}/^4\text{He}$ values have $\delta^{15}\text{N}$ values between 0 and $+3\%$ (refs. 2,4), higher than the values attributed to the convective mantle and similar to both sediments and altered oceanic crust (Extended Data Fig. 1)^{12,13,15,24}. One hypothesis is that the convective and deep mantle reservoirs both initially had identical but low enstatite chondrite-like $\delta^{15}\text{N}$ values⁶. Over geological time, these

¹Department of Earth, Planetary, and Space Sciences, UCLA, Los Angeles, CA, USA. ²Marine Chemistry and Geochemistry Department, Woods Hole Oceanographic Institution, Woods Hole, MA, USA. ³Centre de Recherches Pétrographiques et Géochimiques, CNRS, Université de Lorraine, Vandoeuvre les Nancy, France. ⁴Department of Earth Sciences, University of Toronto, Toronto, Ontario, Canada. ⁵Department of Earth and Planetary Sciences, University of New Mexico, Albuquerque, NM, USA. ⁶Université de Paris, Institut de physique du globe de Paris, CNRS, Paris, France. ⁷Istituto Nazionale di Geofisica e Vulcanologia, Sezione di Palermo, Italy. ⁸Department of Earth Sciences, University of Oxford, Oxford, UK. ⁹Nordvulk, Institute of Earth Sciences, University of Iceland, Reykjavik, Iceland. ¹⁰Thermo Fisher Scientific, Bremen, Germany. ¹¹Present address: Université de Paris, Institut de physique du globe de Paris, CNRS, Paris, France.

[✉]e-mail: labidi@ipgp.fr; eyoung@epss.ucla.edu

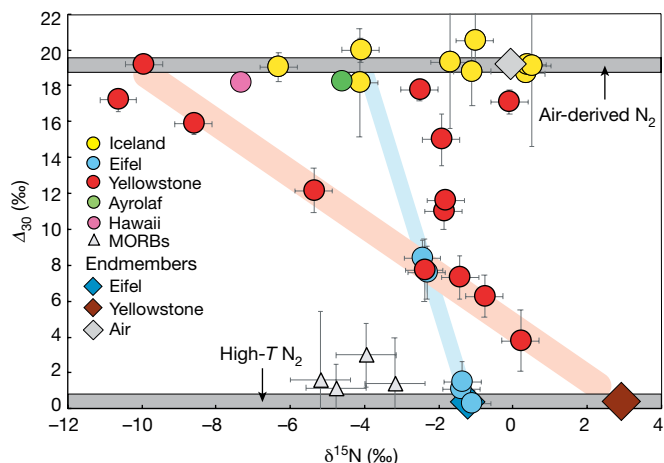


Fig. 1 | The nitrogen isotopic composition of volcanic gases and volatile-rich MORBs. Volcanic gases were collected in hydrothermal systems from Iceland, Hawaii (USA), Yellowstone (Wyoming, United States), Ayrolaf (Ethiopia) and Eifel (Germany). MORBs are popping glasses from the Mid-Atlantic Ridge. Data can be found in Supplementary Table 1. Error bars are 2σ and their magnitude is a function of counting statistics. The nitrogen isotopic and isotopologue compositions of air are shown. Atmospheric N_2 has a known Δ_{30} of $+19.1 \pm 0.3\text{‰}$ (2 s.d.), relative to high-temperature nitrogen with $\Delta_{30} = 0\text{‰}$ (ref. ²⁵). Icelandic samples have exclusively air-derived N_2 as shown by atmospheric Δ_{30} values. The varying $\delta^{15}\text{N}$ values at any given atmospheric Δ_{30} value are evidence for isotopic fractionation of air-derived N_2 in the geothermal system. Similar fractionation is observed in the gases from all of the investigated locations. Since high-temperature nitrogen has by definition a Δ_{30} of 0‰ , mixing relationships can be confidently extrapolated to this value along straight lines. This allows the endmember $\delta^{15}\text{N}$ of the degassing magmas to be determined from volcanic gases. Shaded areas demarcate the mixing trends defined by the data for Eifel (blue) and Yellowstone (red). We find that Eifel and Yellowstone gases have mantle-derived $\delta^{15}\text{N}$ values of -1.4 and $+3\text{‰}$, respectively. Note that the Yellowstone data are also affected by a third component resembling air in both Δ_{30} and $\delta^{15}\text{N}$ values.

reservoirs would have both received nitrogen entrained from the surface by subduction of sediments^{2,4,6} with $\delta^{15}\text{N}$ values of approximately $+3\text{‰}$ (refs. ^{12–15}) (Extended Data Fig. 1). The accumulation of subducted sediment in plume sources would have overwhelmed the primordial bulk nitrogen such that the plume sources acquired the $^{15}\text{N}/^{14}\text{N}$ values of the recycled surface components⁶. Because the convective mantle has negative $\delta^{15}\text{N}$ values of $-5 \pm 3\text{‰}$, it is thought to have received proportionally less recycled nitrogen⁶. The importance of surface nitrogen accumulation in the mantle is uncertain in part because the nitrogen concentrations in mantle reservoirs are poorly known¹.

Here, we eliminate some of the pervasive uncertainties associated with the deep nitrogen cycle by deriving $\delta^{15}\text{N}$, $N_2/{}^3\text{He}$ and $N_2/{}^{36}\text{Ar}$ values of gases from Yellowstone, Iceland and Eifel magmas. In the mantle sources, the elemental ratios vary as a direct result of nitrogen addition to the mantle, since mantle ${}^3\text{He}$ and perhaps a substantial fraction of ${}^{36}\text{Ar}$ are primordial, being vestiges of the accretion of Earth, and thus have fixed concentrations. We use hydrothermal gases, which are more plentiful than the small quantities of gas accessible from mantle-derived rocks. However, these gases have historically shown even greater air contamination than basalts⁹ and for this reason their $^{15}\text{N}/^{14}\text{N}$ ratios are ambiguous⁷. We disentangle the contributions of air and mantle N_2 using a new isotopologue approach in which we determine the abundances of $^{15}\text{N}^{15}\text{N}$ in volcanic N_2 gases. We use the $^{15}\text{N}^{15}\text{N}$ concentration relative to a random distribution of ^{14}N and ^{15}N atoms among N_2 molecules, Δ_{30} , as an unambiguous tracer of air contamination. The Δ_{30} tracer is defined as $\Delta_{30} = {}^{30}\text{R}/({}^{15}\text{R})^2 - 1$ (‰), where ${}^{30}\text{R} = {}^{15}\text{N}^{15}\text{N}/{}^{14}\text{N}^{14}\text{N}$ and ${}^{15}\text{R} = {}^{15}\text{N}/{}^{14}\text{N}$ for the gas of interest²⁵. At relevant temperatures ranging from 200 to 1,000 °C, equilibrium among N_2 isotopologues results in

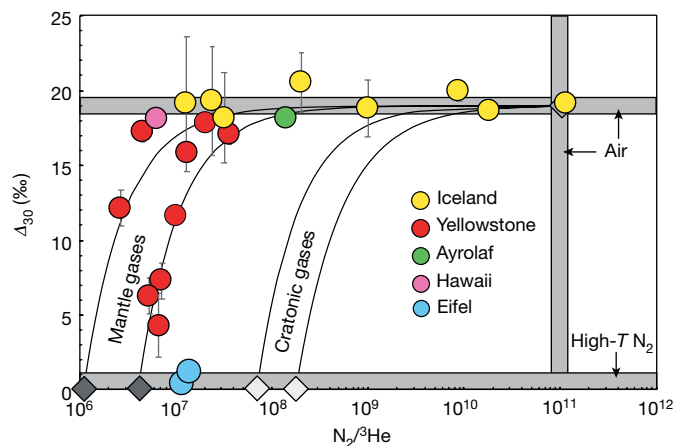


Fig. 2 | The relationship between Δ_{30} and $N_2/{}^3\text{He}$ ratios in volcanic gases. Δ_{30} and $N_2/{}^3\text{He}$ ratios are shown for samples collected at the same time from gases in Iceland, Yellowstone, Hawaii and Ayrolaf. The error bars are 2σ . Data can be found in Supplementary Table 1. Two estimates for mantle gases are shown as the dark grey diamonds with $N_2/{}^3\text{He}$ ratios of 1×10^6 and 4×10^6 , after Marty et al.¹¹. These are consistent with the popping rock estimate¹¹ of $(2.9 \pm 0.1) \times 10^6$. Two estimates for cratonic gases are shown as light grey diamonds. These are derived from our data on cratonic gases from two locations in the Canadian Shield (see Supplementary Information). For $N_2/{}^3\text{He}$ ratios, the cratonic endmembers are 0.7×10^8 and 1.8×10^8 (see Methods for details and Supplementary Table 2 for data). The samples show a clear mixing between air and mantle-derived gases, with a negligible cratonic crustal contribution. Icelandic samples have $N_2/{}^3\text{He}$ ratios ranging down to 10^7 , but no substantial contribution of mantle N_2 is observed. Note that no He concentrations were obtained for Eifel as the samples were collected in glass vials, leading to appreciable He diffusion out of the containers. Existing data obtained with no Δ_{30} measurements suggest a $N_2/{}^3\text{He}$ value below 3.0×10^7 (ref. ¹⁰).

Δ_{30} values from 0.5 to 0.1‰, respectively. An extreme atmospheric Δ_{30} value of $19.1 \pm 0.3\text{‰}$ (2σ) was recently discovered²⁵, providing a robust tracer for air contamination. The remarkable isotopic disequilibrium between atmospheric and high-temperature N_2 is probably due to gas-phase chemistry in the thermosphere²⁵. The atmospheric excess in Δ_{30} provides a powerful tool with which to quantify air-derived N_2 in natural fluids.

Icelandic gases lack atmospheric O_2 , suggesting the absence of air contamination during sampling, although there is no a priori information about the origin of N_2 . The Icelandic gases have ${}^3\text{He}/{}^4\text{He}$ ratios between $8.5R_A$ and $16.3R_A$ (where R_A is the air ${}^3\text{He}/{}^4\text{He}$ ratio), suggesting they tap a mantle plume. These samples have $\delta^{15}\text{N}$ values ranging between those for air (0‰) and the convective mantle (-5‰), while both $N_2/{}^{36}\text{Ar}$ and ${}^{40}\text{Ar}/{}^{36}\text{Ar}$ ratios are air-like, thus leading to confusion regarding the provenance of N_2 (Extended Data Figs. 2, 3). We find that the Icelandic samples have Δ_{30} values ranging between $18.2 \pm 3.0\text{‰}$ and $20.5 \pm 2.0\text{‰}$, with an average of $19.1 \pm 1.2\text{‰}$ —a value that is indistinguishable from the atmospheric value (Fig. 1). This high, air-like Δ_{30} value is markedly different from the values expected from high-temperature nitrogen: by design, Δ_{30} values of -0‰ should characterize N_2 molecules from magmas, because at magmatic temperatures, thermodynamic equilibrium approaches the random distribution of $^{15}\text{N}^{15}\text{N}$ relative to other N_2 isotopologues. We tested this expectation using MORBs with extraordinarily high volatile concentrations (see Methods). Crushing experiments under vacuum released N_2 with $\delta^{15}\text{N}$ values between $-5.2 \pm 1.2\text{‰}$ and $-3.2 \pm 1.5\text{‰}$, similar to conventional MORB values^{3,11}, and Δ_{30} values between $+1.2 \pm 2.6\text{‰}$ and $+3.0 \pm 3.6\text{‰}$ (Fig. 1). Despite large uncertainties due to small sample sizes, our results confirm the prediction that magmatic N_2 formed by degassing at $-1,200$ °C has Δ_{30} values $\sim 0\text{‰}$. The atmospheric Δ_{30} values for the Icelandic gases could represent recycled surface-derived nitrogen in the Icelandic

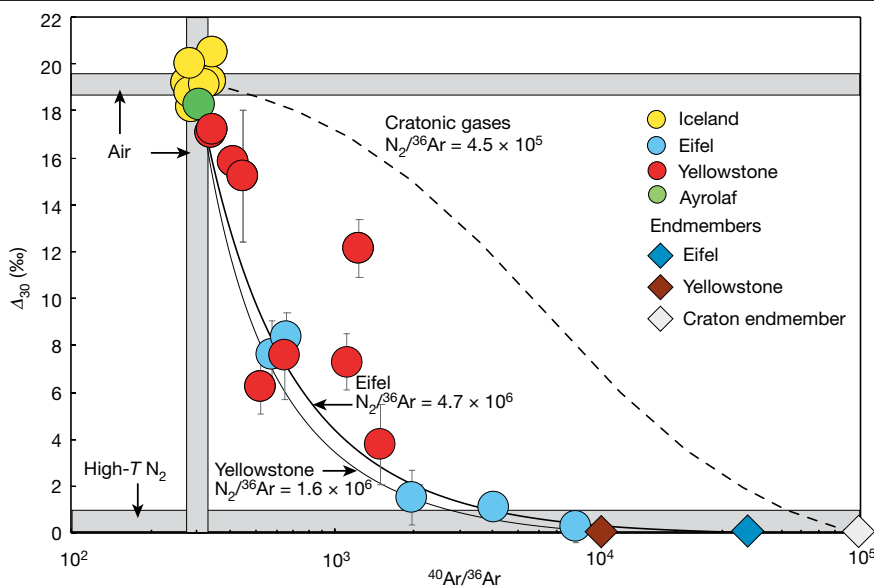


Fig. 3 | The relationship between Δ_{30} and argon isotopes in volcanic gases. Δ_{30} and $^{40}\text{Ar}/^{36}\text{Ar}$ ratios are shown for Iceland, Yellowstone and Eifel gases. The error bars are 2σ . Data can be found in Supplementary Table 1. The data define two-component mixing trends. High- T nitrogen has a fixed Δ_{30} value of 0‰, allowing fitting of the mixing curves to known mantle endmembers. The thick solid curve is the fit for the Eifel samples, calculated with mantle $^{40}\text{Ar}/^{36}\text{Ar}$ and Δ_{30} values of 39,400 (see Methods) and 0‰, respectively. The fit requires a high- T endmember $\text{N}_2/^{36}\text{Ar}$ ratio of 4.7×10^6 . The thin solid curve is a fit for the Yellowstone data, calculated with mantle $^{40}\text{Ar}/^{36}\text{Ar}$ and Δ_{30} values of 10,000

(see Methods) and 0‰, respectively. The best-fit curve corresponds to a $\text{N}_2/^{36}\text{Ar}$ ratio of 1.6×10^6 for the Yellowstone mantle plume. The sole outlier may record crustal input, but this would apply to only that sample. As an illustration of the effects of cratonic crustal inputs, we show a mixing curve between air and cratonic gases with a $^{40}\text{Ar}/^{36}\text{Ar}$ value of 100,000 (dashed curve). In this case, the $\text{N}_2/^{36}\text{Ar}$ is taken to be 4.5×10^5 , the value for the cratonic endmember based on samples from the Superior Province of the Canadian Shield (Kidd Creek gases; see Methods). Despite the proximity of cratonic rocks, none of the samples from Yellowstone have $\text{N}_2/^{3}\text{He}$ ratios consistent with any cratonic input (Fig. 2).

plume²⁶ only if nitrogen was recycled as N_2 molecules, surviving their trip from the surface and the melting process in the mantle intact. However, surface nitrogen is subducted as NH_4^+ ions incorporated into organic matter and within phyllosilicate crystal lattices, rather than as N_2 molecules^{12,14}. Because N_2 is destroyed when nitrogen enters solids, no $^{15}\text{N}/^{14}\text{N}$ atmospheric signature can survive the subduction process.

Atmospheric Δ_{30} values (Fig. 1) unambiguously show that virtually all N_2 in the Icelandic gases from this study is derived from air via contamination within hydrothermal systems. Similar $\delta^{15}\text{N}$ and Δ_{30} values are observed for a sample from the Halemaumau crater (Hawaii) and from a hot spring in Ayrolaf (Ethiopia), indicating a >95% contribution from air-derived N_2 in these fluids as well. These air-like Δ_{30} values unambiguously show that negative $\delta^{15}\text{N}$ values can result from mass-dependent isotope fractionation of atmospheric N_2 occurring in hydrothermal systems, rather than being indicative of a mantle origin. Isotopic fractionation has been invoked previously to account for extremely low $\delta^{15}\text{N}$ values of Icelandic fumaroles⁷. The existence of this fractionation can now be confirmed on the basis of Δ_{30} values. Kinetic dissolution of N_2 in waters leads to enrichments of $\sim 0.5\%$ in ^{14}N in dissolved N_2 at 60 °C (ref. 27). Waters that had degassed 99% of air-derived N_2 in an open system could produce $\delta^{15}\text{N}$ values of around -5% as a result of Rayleigh distillation (see Methods). Degassing of air-saturated water at temperatures of $T > 60$ °C is predicted to cause a negative correlation between $\delta^{15}\text{N}$ and both Kr/Ar and Xe/Ar ratios, as the heavier noble gases are more soluble than argon in water²⁸. This is at odds with the positive correlation observed here (Extended Data Fig. 4), suggesting that degassing from geothermal waters for these samples under non-ideal behaviour—as has been documented under elevated temperatures and pressures ($T > 100$ °C and $P > 20$ bar), where experimental evidence hints at reversals of the Ar to Kr–Xe relative solubilities²⁹.

We also analysed geothermal gases from Yellowstone and Eifel; Δ_{30} values are variable, as low as $3.8 \pm 1.7\%$ and $0.3 \pm 0.6\%$ for Yellowstone and Eifel respectively (Fig. 1). This establishes the contribution of high- T N_2 with $\Delta_{30} \approx 0$, in stark contrast with the Iceland gases (Fig. 1).

Correlations between Δ_{30} and various isotope and element ratios can be extrapolated to $\Delta_{30} = 0$ to constrain magmatic components in mixed gases like those in this study. For Yellowstone, our data constrain high- T N_2 to have a $\delta^{15}\text{N}$ value of $+3 \pm 2\%$ (Fig. 1). This value probably represents the Yellowstone mantle source, and is similar to estimates for Kola and Society^{2,4}. In the case of Eifel, we obtain a high- T N_2 $\delta^{15}\text{N}$ value of $-1.2 \pm 0.5\%$ (Fig. 1), slightly higher than the convective mantle. When Δ_{30} is plotted versus $\text{N}_2/^{3}\text{He}$ (Fig. 2), gas samples define a two-component mixing curve between air with $\text{N}_2/^{3}\text{He} \approx 10^{11}$ and high- T gases with lower $\text{N}_2/^{3}\text{He}$ ratios. An upper limit for $\text{N}_2/^{3}\text{He}$ of $\sim 10^6$ may be obtained for the Iceland plume based on the lowest $\text{N}_2/^{3}\text{He}$ at air-like Δ_{30} values (Fig. 2). This $\text{N}_2/^{3}\text{He}$ ratio is similar to that of the convective mantle¹¹ and is lower by four orders of magnitude than an earlier suggestion derived from extrapolations of Icelandic basalts showing near-atmospheric $^{40}\text{Ar}/^{36}\text{Ar}$ ratios but lacking Δ_{30} measurements²⁶. The Yellowstone samples also define a deep source with $\text{N}_2/^{3}\text{He} \approx 10^6$ (Fig. 2 and Extended Data Fig. 1) with no indication of an elemental fractionation in the hydrothermal system, in agreement with a previous study³⁰. This rules out the possibility of nitrogen assimilation from the crust (see Methods for details). The Eifel samples require a $\text{N}_2/^{3}\text{He}$ value of $\sim 10^7$ for the Eifel source, higher than the convective mantle.

When Δ_{30} is plotted against $^{40}\text{Ar}/^{36}\text{Ar}$ (Fig. 3), data for Iceland are indistinguishable from air. Data for the Eifel and Yellowstone samples exhibit correlations consistent with two-component mixing hyperbolae with curvatures defined by $[\text{N}_2/^{36}\text{Ar}]_{\text{Mantle}}/[\text{N}_2/^{36}\text{Ar}]_{\text{Air}}$. Using an $\text{N}_2/^{36}\text{Ar}$ ratio of 2.5×10^4 for air, we can extrapolate Yellowstone and Eifel data to estimate the $\text{N}_2/^{36}\text{Ar}$ for the mantle feeding both systems. For the Eifel mantle source, we obtain an $\text{N}_2/^{36}\text{Ar}$ value of $4.7^{+0.8}_{-1.6} \times 10^6$ (Fig. 3), marginally higher than the convective mantle value of $2.0^{+1.0}_{-1.2} \times 10^6$ (Extended Data Figs. 1, 5). This, coupled with the high $\delta^{15}\text{N}$ and $\text{N}_2/^{3}\text{He}$ values relative to the convective mantle, suggests a contribution of subducted dehydrated oceanic crust with $\text{N}_2/^{36}\text{Ar} > 10^7$ and $\text{N}_2/^{3}\text{He} > 10^{11}$ of $\sim 30\%$ to the Eifel mantle source (Methods, Extended Data Fig. 6), consistent with a recent noble gas study³¹. The Yellowstone

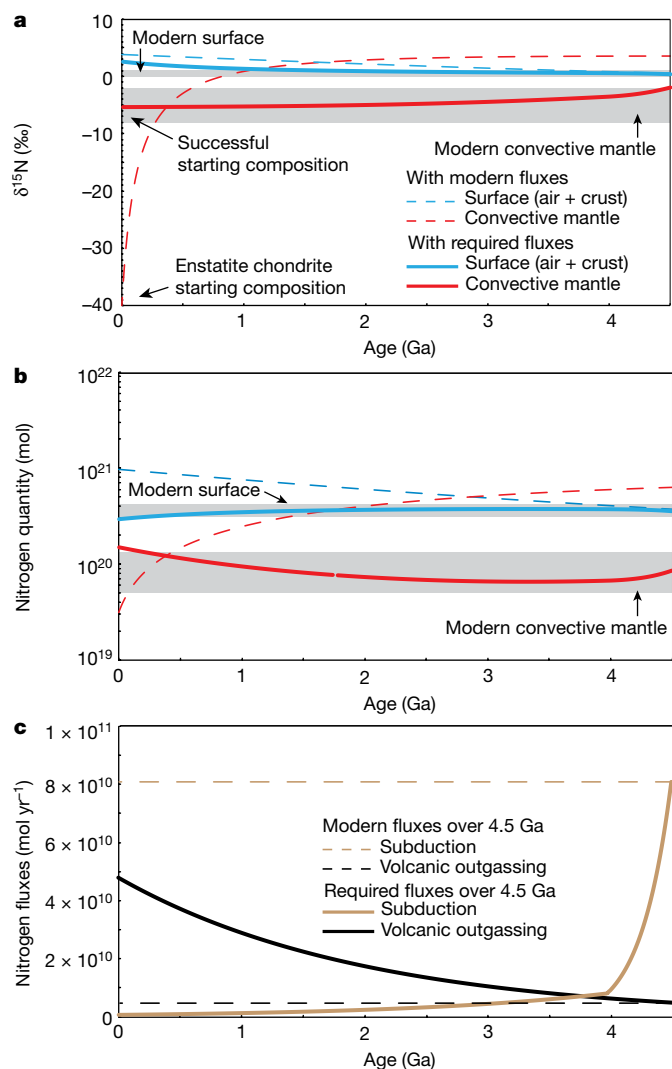


Fig. 4 | The evolution of $\delta^{15}\text{N}$ and nitrogen abundances in the convective mantle and at the Earth's surface as a function of time. **a**, $\delta^{15}\text{N}$ evolution. **b**, Nitrogen abundance. **c**, The rates of N subduction and outgassing used in the model. Required fluxes refer to the example of a successful model, where subduction rates remain lower than volcanic outgassing rates for most of Earth's history. These fluxes evolve over time, with decreasing outgassing and increasing subduction fluxes. With these fluxes, the mantle and surface show limited exchange, and therefore limited isotope evolution (solid curves), as seemingly required by the lack of secular evolution of the surface nitrogen reservoir²⁴. For the mantle, the starting material was chosen to have an enstatite chondrite-like $\delta^{15}\text{N}$ value. Different initial quantities of nitrogen were considered. One scenario is based on 3×10^{19} mol N in the mantle, which corresponds to 0.15 ppm N in the convective mantle, and is an extreme case where the convective mantle corresponds to the full mass of the Earth's mantle (4×10^{27} g). This constitutes the minimum plausible mantle nitrogen concentration estimate⁴. The result of the model is not markedly different if the initial concentration of mantle nitrogen differs by an order of magnitude, as the concentration is rapidly influenced by the subduction flux of nitrogen. A critical result of the model is that if modern rates of outgassing and subduction¹³ applied throughout geological time, nitrogen isotope ratios should have evolved to a steady state in which the mantle has a higher $\delta^{15}\text{N}$ than the surface (dashed curves), contrary to the present-day situation. See Methods for details.

data in Fig. 3 define a $\text{N}_2/^{36}\text{Ar}$ ratio of $1.6_{-0.4}^{+0.7} \times 10^6$ for the plume, indistinguishable from the convective mantle but distinct from previous investigations of plume sources, where ratios of $\sim 10^5$ were suggested^{2,4}. This is evidence that Yellowstone may derive from a ^3He -rich plume

source that has $\text{N}_2/^{36}\text{Ar}$ and $\text{N}_2/^{36}\text{Ar}$ ratios indistinguishable from the convective mantle but a $\delta^{15}\text{N}$ value that is as high as that of nitrogen in subducting slabs (Extended Data Fig. 1).

To investigate the implications of our results for the potential $\text{N}_2/^{36}\text{Ar}$, $\text{N}_2/^{36}\text{He}$ and $\delta^{15}\text{N}$ values of sediment-bearing slabs recycled into the mantle, we calculated mixing curves between the convective mantle and recycled components with various $\delta^{15}\text{N}$ values (Extended Data Fig. 6). We consider that $\text{N}_2/^{36}\text{Ar}$ and $\text{N}_2/^{36}\text{He}$ ratios of slabs recycled into the mantle could be as high as $\sim 10^7$ and $\sim 10^{12}$, respectively^{26,32}. We find that mixing successfully accounts for ^3He -poor Eifel data, as well as for previous data from the ^3He -poor Society plume⁴, where high $\text{N}_2/^{36}\text{He}$ values of $\sim 10^7$ and $\sim 10^9$, respectively, may reflect nitrogen addition via subduction. Variable $\text{N}_2/^{36}\text{Ar}$ ratios for these systems^{2,4} could be caused by fractionations in the slabs. In contrast, mixing fails to account for the Yellowstone data unless recycled slabs have $\delta^{15}\text{N} > 50\%$, an implausibly high value given the data for sediments, or unless the ^3He -rich mantle source is forced to have arbitrarily low $\text{N}_2/^{36}\text{Ar}$ and $\text{N}_2/^{36}\text{He}$ ratios of $\leq 2 \times 10^5$ (Methods, Extended Data Fig. 6). In the latter case, the similarity in $\text{N}_2/^{36}\text{Ar}$ and $\text{N}_2/^{36}\text{He}$ ratios between Yellowstone gases and the convective mantle would be purely serendipitous, an unlikely result arising only from mixing two disparate components in just the right proportions to yield convective mantle values.

In view of these new data, subduction may not be the simplest scenario to account for high $\delta^{15}\text{N}$ values in the ^3He -rich Yellowstone mantle source (see Methods), and more $^{15}\text{N}/^{14}\text{N}$ data for other ^3He -rich plumes will help address this question. In the interim, and motivated by these initial $^{15}\text{N}/^{14}\text{N}$ results, we provide a computational test of the general hypothesis that subduction of surface-derived nitrogen controls mantle nitrogen isotope ratios at the global scale^{2,4,6}. We test whether subduction could shift the $\delta^{15}\text{N}$ signature of a once chondritic mantle (enstatite or other type of chondrite) to the modern value of $-5 \pm 3\%$ (refs. ^{11,15}) over geological time. If this hypothesis is correct, the relative distribution of nitrogen between the mantle and surface reservoirs requires that the $\delta^{15}\text{N}$ values for both varied with time. We calculate the time evolution of both the mass of nitrogen and the $^{15}\text{N}/^{14}\text{N}$ ratios for Earth's mantle and surface using a two-box model (Methods). We fit the approximate mantle nitrogen concentration of 0.3 ppm (ref. ⁴) to within an order of magnitude, but considerably higher mantle concentrations of nitrogen¹ would not change the result (Fig. 4). We take modern rates of nitrogen subduction to be greater than rates of outgassing at mid-ocean ridges by an order of magnitude¹³. Extrapolating these rates back over geological timescales results in the global nitrogen cycle reaching an isotopic steady state in which the mantle has a higher $\delta^{15}\text{N}$ value than that for the surface by 3%, regardless of the starting $\delta^{15}\text{N}$ values (Fig. 4). In this model, it is straightforward to show that, at steady state, the mantle $^{15}\text{N}/^{14}\text{N}$ isotope ratio is:

$$\frac{n_{^{15}\text{N}}^{\text{Mantle}}}{n_{^{14}\text{N}}^{\text{Mantle}}} = \frac{\alpha_{\text{sub}}(k_{\text{sub}} + k_{\text{vol}})}{\alpha_{\text{sub}}k_{\text{sub}} + k_{\text{vol}}} \left(\frac{^{15}\text{N}}{^{14}\text{N}} \right)_{\oplus} \quad (1)$$

where $n_{i\text{N}}^j$ refers to the extensive quantity of nitrogen isotope i (for example, moles of ^{14}N) in reservoir j , $(^{15}\text{N}/^{14}\text{N})_{\oplus}$ is the bulk Earth nitrogen isotope ratio, k_{sub} and k_{vol} are rate constants (yr^{-1}) for subduction and volcanism, respectively, and $\alpha_{\text{sub}} = (^{15}\text{N}/^{14}\text{N})_{\text{sub}} / (^{15}\text{N}/^{14}\text{N})_{\text{surface}}$ is the isotope fractionation factor relating the isotopic composition of subducted nitrogen to that of the average surface. When $k_{\text{sub}} \gg k_{\text{vol}}$, as suggested by present-day fluxes, the mantle acquires and retains virtually all of Earth's nitrogen and because $\alpha_{\text{sub}} = 1.003$ (refs. ^{13,14,24}), surface nitrogen tends towards $^{15}\text{N}/^{14}\text{N}$ ratios lower than the mantle value. Furthermore, the prolonged exchange of nitrogen between Earth's surface and the convective mantle forces the mantle $^{15}\text{N}/^{14}\text{N}$ value to be greater than that of the surface reservoir by a factor of $\alpha_{\text{sub}} \approx 1.003$ (Fig. 4). The fact that subduction of nitrogen should eventually cause $(^{15}\text{N}/^{14}\text{N})_{\text{Mantle}} > (^{15}\text{N}/^{14}\text{N})_{\text{Surface}}$ and yet the opposite is observed today places important constraints on the nature of the surface–mantle exchange of nitrogen

over geological time. This simple, but seemingly inescapable, conclusion implies that the nitrogen cycle is not at steady state⁴ and that the fluxes observed today are not indicative of those in the past.

Non-steady-state scenarios were explored to match the present-day nitrogen concentrations and $\delta^{15}\text{N}$ values of air and convective mantle by varying fluxes and initial $\delta^{15}\text{N}$ values (Extended Data Fig. 7). The time-dependent solutions not only require considerable secular evolution of the surface $\delta^{15}\text{N}$ value that is inconsistent with observations^{24,33}, but they also demand ad hoc pairings of initial compositions and fluxes. The simplest solution to satisfy modern observations is if mantle and surface initial $\delta^{15}\text{N}$ values are $-6 \pm 4\%$ and $0.5 \pm 1.5\%$, respectively (Fig. 4), and if subduction N fluxes are substantially lower than volcanic nitrogen outgassing fluxes throughout most of Earth's history ($k_{\text{sub}} \ll k_{\text{vol}}$). This scenario would require the net degassing of $\sim 3 \times 10^{19}$ mol N_2 over Earth's history, which represents only $\sim 20\%$ of the N_2 quantity in the modern-day atmosphere. Overall limited exchange also prevents nitrogen isotopic evolution for both the mantle and the surface over geological time (Fig. 4). Low subduction fluxes of nitrogen to the mantle can be explained if nitrogen was lost from downgoing slabs in subduction zones with high thermal gradients^{8,12,14,15}, as appears more likely during the Archaean and Proterozoic eons. A corollary is that the convective mantle must have remained largely unaffected by subducted nitrogen, in contrast with earlier conclusions^{4–6}.

Work is needed to elucidate the $\delta^{15}\text{N}$ difference between the convective mantle and ^3He -rich reservoirs, but we suggest that it may reflect $^{15}\text{N}/^{14}\text{N}$ fractionation processes within the mantle as recorded in peridotite diamonds¹⁸, or a varying $^{15}\text{N}/^{14}\text{N}$ fractionation between the deep silicate mantle and iron-rich metal during core formation, as suggested by some experiments^{21,22}. We conclude that $\delta^{15}\text{N}$ can be a deceptive tracer of nitrogen provenance not only in hydrothermal gases, but also in mantle sources. We suggest that Δ_{30} can be used to eliminate the confounding effects of contamination by air in volcanic gases, and as a vehicle for extracting mantle endmember isotopic compositions from gas data.

Online content

Any methods, additional references, Nature Research reporting summaries, source data, extended data, supplementary information, acknowledgements, peer review information; details of author contributions and competing interests; and statements of data and code availability are available at <https://doi.org/10.1038/s41586-020-2173-4>.

1. Javoy, M. The birth of the Earth's atmosphere: the behaviour and fate of its major elements. *Chem. Geol.* **147**, 11–25 (1998).
2. Dauphas, N. & Marty, B. Heavy nitrogen in carbonatites of the Kola Peninsula: a possible signature of the deep mantle. *Science* **286**, 2488–2490 (1999).
3. Marty, B. & Zimmermann, L. Volatiles (He, C, N, Ar) in mid-ocean ridge basalts: assessment of shallow-level fractionation and characterization of source composition. *Geochim. Cosmochim. Acta* **63**, 3619–3633 (1999).
4. Marty, B. & Dauphas, N. The nitrogen record of crust–mantle interaction and mantle convection from Archaean to Present. *Earth Planet. Sci. Lett.* **206**, 397–410 (2003).
5. Palot, M., Cartigny, P., Harris, J. W., Kaminsky, F. V. & Stachel, T. Evidence for deep mantle convection and primordial heterogeneity from nitrogen and carbon stable isotopes in diamond. *Earth Planet. Sci. Lett.* **357–358**, 179–193 (2012).
6. Barry, P. H. & Hilton, D. R. Release of subducted sedimentary nitrogen throughout Earth's mantle. *Geochim. Perspect. Lett.* **2**, 148–159 (2016).
7. Marty, B. et al. Gas geochemistry of geothermal fluids, the Hengill area, southwest rift zone of Iceland. *Chem. Geol.* **91**, 207–225 (1991).

8. Fischer, T. P. et al. Subduction and recycling of nitrogen along the Central American margin. *Science* **297**, 1154–1157 (2002).
9. Fischer, T. et al. Upper-mantle volatile chemistry at Oldoinyo Lengai volcano and the origin of carbonatites. *Nature* **459**, 77–80 (2009).
10. Bräuer, K., Kämpf, H., Niedermann, S. & Strauch, G. Indications for the existence of different magmatic reservoirs beneath the Eifel area (Germany): a multi-isotope (C, N, He, Ne, Ar) approach. *Chem. Geol.* **356**, 193–208 (2013).
11. Javoy, M. & Pineau, F. The volatiles record of a “popping” rock from the Mid-Atlantic Ridge at 14°N : chemical and isotopic composition of gas trapped in the vesicles. *Earth Planet. Sci. Lett.* **107**, 598–611 (1991).
12. Bebout, G. E. & Fogel, M. L. Nitrogen-isotope compositions of metasedimentary rocks in the Catalina Schist, California: implications for metamorphic devolatilization history. *Geochim. Cosmochim. Acta* **56**, 2839–2849 (1992).
13. Busigny, V., Cartigny, P. & Philippot, P. Nitrogen isotopes in ophiolitic metagabbros: a re-evaluation of modern nitrogen fluxes in subduction zones and implication for the early Earth atmosphere. *Geochim. Cosmochim. Acta* **75**, 7502–7521 (2011).
14. Busigny, V., Cartigny, P., Philippot, P., Ader, M. & Javoy, M. Massive recycling of nitrogen and other fluid-mobile elements (K, Rb, Cs, H) in a cold slab environment: evidence from HP to UHP oceanic metasediments of the Schistes Lustrés nappe (western Alps, Europe). *Earth Planet. Sci. Lett.* **215**, 27–42 (2003).
15. Bebout, G. E., Agard, P., Kobayashi, K., Moriguti, T. & Nakamura, E. Devolatilization history and trace element mobility in deeply subducted sedimentary rocks: evidence from Western Alps HP/UHP suites. *Chem. Geol.* **342**, 1–20 (2013).
16. Grady, M. & Wright, I. Elemental and isotopic abundances of carbon and nitrogen in meteorites. *Space Sci. Rev.* **106**, 231–248 (2003).
17. Abernethy, F. A. J. et al. Stable isotope analysis of carbon and nitrogen in angrites. *Meteorit. Planet. Sci.* **48**, 1590–1606 (2013). We include issue numbers in journal references only when each issue begins at page 1; the issue number has therefore been removed from ref. 17.
18. Cartigny, P., Palot, M., Thomassot, E. & Harris, J. W. Diamond formation: a stable isotope perspective. *Annu. Rev. Earth Planet. Sci.* **42**, 699–732 (2014).
19. Pearson, V. K., Sephton, M. A., Franchi, I. A., Gibson, J. M. & Gilmour, I. Carbon and nitrogen in carbonaceous chondrites: elemental abundances and stable isotopic compositions. *Meteorit. Planet. Sci.* **41**, 1899–1918 (2006).
20. Young, E. D. et al. Near-equilibrium isotope fractionation during planetesimal evaporation. *Icarus* **323**, 1–15 (2019).
21. Li, Y., Marty, B., Shcheka, S., Zimmermann, L. & Keppler, H. Nitrogen isotope fractionation during terrestrial core–mantle separation. *Geochim. Perspect. Lett.* **2**, 138–147 (2016).
22. Dalou, C. et al. Redox control on nitrogen isotope fractionation during planetary core formation. *Proc. Natl Acad. Sci. USA* **116**, 14485–14494 (2019).
23. Allègre, C. J. & Turcotte, D. L. Implications of a two-component marble-cake mantle. *Nature* **323**, 123–127 (1986).
24. Thomazo, C. & Papineau, D. Biogeochemical cycling of nitrogen on the early Earth. *Elements* **9**, 345–351 (2013).
25. Yeung, L. Y. et al. Extreme enrichment in atmospheric $^{15}\text{N}/^{14}\text{N}$. *Sci. Adv.* **3**, ea06741 (2017).
26. Halldórsson, S. A., Hilton, D. R., Barry, P. H., Füre, E. & Grönvold, K. Recycling of crustal material by the Iceland mantle plume: new evidence from nitrogen elemental and isotope systematics of subglacial basalts. *Geochim. Cosmochim. Acta* **176**, 206–226 (2016); corrigendum 186, 360–364 (2016).
27. Lee, H., Sharp, Z. D. & Fischer, T. P. Kinetic nitrogen isotope fractionation between air and dissolved N_2 in water: implications for hydrothermal systems. *Geochem. J.* **49**, 571–573 (2015).
28. Ballentine, C. J., Burgess, R. & Marty, B. Tracing fluid origin, transport and interaction in the crust. *Rev. Mineral. Geochem.* **47**, 539–614 (2002).
29. Warr, O., Rochelle, C. A., Masters, A. & Ballentine, C. J. Determining noble gas partitioning within a CO_2 – H_2O system at elevated temperatures and pressures. *Geochim. Cosmochim. Acta* **159**, 112–125 (2015).
30. Chiodini, G. et al. Insights from fumarole gas geochemistry on the origin of hydrothermal fluids on the Yellowstone Plateau. *Geochim. Cosmochim. Acta* **89**, 265–278 (2012).
31. Bekaert, D. V. B., Broadley, M. W., Caracausi, A. & Marty, B. Novel insights into the degassing history of the Earth's mantle from high precision noble gas analysis of magmatic gas. *Earth Planet. Sci. Lett.* **525**, 115766–115778 (2019).
32. Sano, Y., Takahata, N., Nishio, Y., Fischer, T. P. & Williams, S. N. Volcanic flux of nitrogen from the Earth. *Chem. Geol.* **171**, 263–271 (2001).
33. Avicé, G. et al. Evolution of atmospheric xenon and other noble gases inferred from Archaean to Paleoproterozoic rocks. *Geochim. Cosmochim. Acta* **232**, 82–100 (2018).

Publisher's note Springer Nature remains neutral with regard to jurisdictional claims in published maps and institutional affiliations.

© The Author(s), under exclusive licence to Springer Nature Limited 2020

Methods

Samples and nitrogen isotope measurements

Samples studied in the volcanic regions of Iceland, Eifel, Yellowstone, Hawaii and Ethiopia come from either dry gases or bubbling springs, and some were collected in high-pressure boreholes (especially samples from Iceland; see data in Supplementary Table 1). We see no systematic difference in the nitrogen isotope systematics across sample types or fluid temperatures during collection. The gases are typically dominated by CO₂. For 22 samples, we collected and stored free gas in 15 cm³ copper tubes. For these samples, the N₂ concentrations vary from 0.1 to 67 vol%, with a mean and median value of 4 vol% and 0.3 vol%, respectively. For all other samples, we used the Giggenbach sampling method to concentrate N₂ and noble gases. For these, we used 200 cm³ glass flasks filled with 50–80 cm³ of 7 M NaOH solution³⁴. The solution titrates reactive gases (water vapour, CO₂, SO₂, H₂S, HCl, HF), allowing non-reactive gases to accumulate (N₂, H₂, O₂, CO, hydrocarbons and noble gases) in the headspace volume. Gases from the continental crust (see below) were collected from exploration boreholes in an underground mine in the Superior Province of the Canadian Shield following the method outlined by Sherwood Lollar et al.³⁵.

N₂ gases were purified by cryogenic separation followed by gas chromatography at the University of California, Los Angeles (UCLA). N₂ concentrations were measured via manometry before mass spectrometric analysis. Isotopologue abundances of N₂ are determined from the ion currents for ¹⁴N¹⁴N⁺, ¹⁴N¹⁵N⁺ and ¹⁵N¹⁵N⁺ with cardinal mass/charge (*m/z*) values of 28, 29 and 30, respectively. The measurements were performed on the Nu Instruments Panorama mass spectrometer at UCLA. Ions with *m/z* ratios of ~30 are detected using a secondary electron multiplier, while the other ions are measured using Faraday cups with 10¹¹ Ω amplifier resistors. A mass-resolving power of roughly 50,000 allowed ¹⁵N¹⁵N⁺ to be resolved from the ¹⁴N¹⁶O⁺ isobaric interference. See detailed methods elsewhere³⁶. Samples with abundant N₂ are analysed for 7.5 h, yielding a typical Δ₃₀ internal precision of 0.1‰ (1σ). Gases have a range of N₂ concentrations (see below), and counting times were adjusted according to the extracted N₂ amounts. For samples with the lowest N₂ quantities (between 1 and 4 μmol N₂), total counting times were less than 1 h, leading to a Δ₃₀ internal precision of typically 1‰ or better. We performed measurements of air standards on 1–3 μmol N₂, mimicking the N₂ amounts extracted from most gases (see Supplementary Table 3). These yielded average Δ₃₀ values of 19.2 ± 0.8‰ (2 s.d., *n* = 7). For air N₂ quantities between 0.5 and 0.1 μmol, the average Δ₃₀ is 19.2 ± 2.1‰ (2 s.d., *n* = 5). Both sets of data are statistically indistinguishable from the earlier value for air from this laboratory of 19.2 ± 0.3‰ (2 s.d., *n* = 11)²⁵. Note that N₂ procedural blanks are 0.005 μmol or less. The data establish the accuracy for Δ₃₀ measurements, down to low quantities of N₂, with larger uncertainties reflecting counting statistics.

Noble gas measurements

Noble gas analyses were conducted in multiple laboratories (see Supplementary Table 1), including at the University of Oxford (UK), the University of New Mexico (United States) and the Istituto Nazionale di Geofisica e Vulcanologia, Sezione di Palermo (Italy) and Le Centre de Recherches Pétrographique et Géochemique (France). The measurement methods are described in detail elsewhere^{37–39}. Briefly, at Oxford, the measurements were performed using a dual mass spectrometer set-up, interfaced with a dedicated extraction and purification system. Gases were introduced to a titanium sponge held at 950 °C for the removal of active gas species. The purified noble gases were then concentrated in a series of cryogenic traps: the sample was first expanded to an all-stainless-steel trap held at an indicative temperature of 15 K. We experimentally established that no Ne or He was adsorbed in these conditions. Following complete adsorption of Ar, the remaining gas was expanded onto a charcoal trap held at approximately 15 K, where

He and Ne were quantitatively adsorbed. The charcoal and all-stainless-steel traps were isolated by a valve. The temperature of the charcoal trap was then raised to 34 K to ensure complete release of He, while all Ne remained adsorbed on the charcoal trap. The He was inlet into a Helix SFT mass spectrometer. Following He abundance and isotope determination, the temperature on the charcoal cryogenic trap was raised to 90 K for 15 min to release Ne, which was inlet into an ARGUS VI mass spectrometer. Following Ne isotope measurement, the all-stainless-steel cryogenic trap temperature was raised to 200 K and Ar isotopes were measured. Both cryogenic traps were empirically calibrated to ensure complete trapping and separation at the aforementioned temperatures. Ar isotope data for the Eifel samples were acquired at the Centre de Recherches Pétrographique et Géochemique (Nancy, France) and are published elsewhere³¹. For gases collected in the Canadian Shield, inorganic gas components (such as N₂, He, Ar) were separated and measured on a TCD gas chromatograph (Varian 3800 GC) using a 5 Å molecular sieve PLOT fused silica column (0.53 mm outer diameter × 25 m length) as outlined in earlier work^{40,41}. All gas samples are measured in triplicate, and uncertainties are ±5% by volume.

Fractionation of air δ¹⁵N in the hydrothermal system

For the Iceland gases, we observe varying δ¹⁵N at a given atmospheric Δ₃₀ value and N₂/³⁶Ar ratio (Supplementary Table 1). Because N₂/³⁶Ar ratios remain air-like at a varying δ¹⁵N, fractionation of nitrogen isotopes during gas migration⁴² is considered unlikely. Dissolution of N₂ in water leads to a kinetic isotope fractionation, and produces depletions of ~0.5‰ in ¹⁵N/¹⁴N in dissolved N₂ at 60 °C (ref.²⁷). Because it probably occurs far from ideal Henry's Law behaviour (for example, Extended Data Fig. 4), the relative equilibrium solubilities of N₂ and ³⁶Ar may not apply²⁹. We suggest that repeated N₂ degassing with associated kinetic isotope fractionation will leave waters with residual N₂ that is increasingly depleted in ¹⁵N. In other words, dissolved N₂ will show decreasing δ¹⁵N. We use the conventional Rayleigh distillation equation and measured dissolved N₂ versus air isotope fractionation²⁷ to calculate that a loss of ~99% N₂ from geothermal waters would be required to account for the observed δ¹⁵N values of around -5‰ with air-like Δ₃₀ values. Much greater losses or larger fractionations are required to account for the Yellowstone samples with δ¹⁵N near -10‰ (Fig. 1), or for data previously acquired on Icelandic geothermal fields⁷.

Preservation of Δ₃₀ in hydrothermal systems

We use Δ₃₀ variations in volcanic gases as measures of the proportions of air and high-*T* N₂ in dinitrogen gas samples. This assumes that atmospheric ¹⁵N/¹⁵N excesses are not re-equilibrated during N₂ storage in aquifers. This assumption is consistent with the known preservation of atmospheric Δ₃₀ values in seawater N₂ (ref.²⁵). At typical seawater temperatures of between 0 and 10 °C, Δ₃₀ is predicted to be 1.4 to 1.1‰ at thermodynamic equilibrium. Preservation of atmospheric Δ₃₀ values shows that N₂ dissolution in water does not reorder ¹⁵N/¹⁵N towards thermodynamic equilibrium. However, high-*T* environments of hydrothermal system (*T* > 100 °C at depth) could, in principle, isotopically reorder N₂ molecules towards a low Δ₃₀ value, reflecting equilibrium at the higher temperatures. At 100 °C, Δ₃₀ is predicted to be 0.75‰ at thermodynamic equilibrium, more than 18‰ lower than the atmospheric ¹⁵N/¹⁵N excess. However, earlier experimental work shows that N₂ isotopologue abundances reorder at high *T* only if heated to >400 °C while in contact with strontium nitride²⁵. Here, we report results of experiments in which N₂ is heated in the laboratory with no nitride catalysts as an attempt to simulate possible re-equilibration in high-*T* hydrothermal and rock-rich systems.

We conducted two series of experiments showing that heated N₂ does not deviate from an initial ¹⁵N/¹⁵N enrichment even after ~3 months at 800 °C. Pure N₂ at a pressure of 0.1 bar was loaded into a sealed quartz tube (19 cm³) that had been previously evacuated. The sample was heated at 800 °C for between 1 and 69 days. The heated N₂ yielded

average Δ_{30} and $\delta^{15}\text{N}$ values of 19.2 ± 0.2 and $-0.6 \pm 0.2\%$ respectively, indistinguishable from the initial Δ_{30} and $\delta^{15}\text{N}$ values of $19.2 \pm 0.2\%$ and $-0.4 \pm 0.1\%$ respectively. In a second set of experiments, N_2 was expanded into a quartz tube containing 2 g of basalt powder (<68 μm mesh). The natural basalt powder considerably increased the potential reaction surfaces between gases and solids. The N_2 plus basalt powder was heated at 800 °C for up to 38 days. In these experiments, N_2 yielded average Δ_{30} and $\delta^{15}\text{N}$ values of 19.0 ± 0.2 and $-0.4 \pm 0.2\%$, respectively. We thus conclude that atmospheric N_2 with a $^{15}\text{N}^{15}\text{N}$ excess is most probably not reordered in natural systems, where nitrides are not in contact with atmosphere-derived gases.

Degassed N_2 from basalts

So-called popping basalt glasses have remarkably high vesicularities (>5 vol%) and are thought to represent melts that have nucleated vesicles containing most of the magmatic volatile budget, but have not lost their bubbles^{11,43,44}. These samples are rare, but their extraordinarily high volatile concentrations permit the investigation of the composition of mantle gases. We investigated the composition of gases trapped in three popping glasses. One was sampled at the Mid-Atlantic Ridge, at 26° N, during cruise KN207-2 of the R/V *Knorr* in June 2012⁴⁵, and two were sampled at the Mid-Atlantic ridge, at 14° N, during cruise AT33-03 in June 2016^{46,47}. We crushed 0.2–2.5 g of glass under vacuum, in a 50 cm³ automated apparatus connected to a vacuum purification line. The pressure increased during crushing from baseline to a plateau value after 1–10 min of continuous crushing. In our extractions, the N_2 fraction was 0.15–0.30 vol%, and the CO_2 fraction was >99 vol%, in agreement with the composition of 2 π D43, the renowned popping glass analysed in previous studies¹¹. We analysed the extracted CO_2 on a MAT 253 gas-source mass spectrometer at UCLA and obtained an average $\delta^{13}\text{C}$ value of $-3.6 \pm 0.2\%$ relative to the Vienna PeeDee Belemnite, consistent with mantle estimates⁴⁸. Only 0.05–0.8 μmol N_2 was extracted, which by necessity yielded the nitrogen isotope measurements with the largest uncertainties reported as part of this study. We obtained $\delta^{15}\text{N}$ values between $-5.2 \pm 1.2\%$ and $-3.2 \pm 1.5\%$, similar to 2 π D43¹¹ and other MORBs^{3,49}, and Δ_{30} values between $+1.2 \pm 2.6\%$ and $+3.0 \pm 3.6\%$ (see Supplementary Table 1). Despite the large uncertainty due to sample size, this estimate is consistent with the prediction based on the thermodynamic equilibrium distribution of N_2 isotopologues that magmatic N_2 should have $\Delta_{30} \approx 0\%$ since it forms by degassing at temperatures as high as $-1,200$ °C. This confirms that magmatic N_2 degassed during eruption carries no $^{15}\text{N}^{15}\text{N}$ enrichment relative to thermodynamic predictions.

Icelandic geothermal gases

Eleven gases from Iceland were collected in 2015, 2016 and 2017. The gases have no detectable atmospheric O_2 , showing they were not contaminated with air during sample collection. Their noble gas compositions fall in the range of Icelandic geothermal gases, as reported in a previous study⁵⁰. The compositional variation in Icelandic geothermal gases is shown in Extended Data Fig. 2, where $^3\text{He}/^4\text{He}$ ratios are plotted against $^4\text{He}/^{20}\text{Ne}$. Both ratios are normalized to air, such that, by design, air is defined by a $^3\text{He}/^4\text{He}$ of $1R_A$ and a $(^4\text{He}/^{20}\text{Ne})/(^4\text{He}/^{20}\text{Ne})_{\text{air}}$ of 1. Literature data⁵⁰ show that the gases can be explained as mixtures of air, the convective mantle and the plume mantle (Extended Data Fig. 2). The convective mantle endmember is characterized by $^3\text{He}/^4\text{He}$ of $\sim 8R_A$ and a relatively high $^4\text{He}/^{20}\text{Ne}$ relative to air of $>10^3$ (ref⁴⁴). The plume component is characterized by primordial $^3\text{He}/^4\text{He}$ ratios of up to $\sim 30R_A$ and a $^4\text{He}/^{20}\text{Ne}$ value lower than the convective mantle^{50,51}. In Extended Data Fig. 2, our 11 samples have compositions that seemingly show contributions from all three Icelandic endmembers.

We show that nitrogen with negative $\delta^{15}\text{N}$ values is in fact derived from air, as illustrated by atmospheric Δ_{30} values (Fig. 1), and not the convective mantle. Some positive $\delta^{15}\text{N}$ values were also observed in apparently air-contaminated Icelandic basalts ($^{40}\text{Ar}/^{36}\text{Ar} < 1,000$)²⁶, and

these were taken as evidence for a recycled crustal component in the plume. However, based on our study, it is possible that the positive $\delta^{15}\text{N}$ values in air-contaminated basalts represent fractionated air as well. This was suggested to explain the positive and negative $\delta^{15}\text{N}$ values of air-contaminated MORBs ($^{40}\text{Ar}/^{36}\text{Ar} < 1,000$) erupted on the seafloor³. It is clear that Δ_{30} data in future work will help constrain the true $\delta^{15}\text{N}$ of the plume component in Iceland.

Eifel spring gases

The $\delta^{15}\text{N}$ value derived for the Eifel mantle endmember, -1.4% , is intermediate between the values for MORB (approximately -5%) and estimates for plumes ($+3\%$)²⁻⁴. The $\text{N}_2/^{36}\text{Ar}$ value derived for Eifel is $4.7_{-1.6}^{+0.8} \times 10^6$, marginally higher than the convective MORB mantle value of $2.0_{-1.0}^{+1.0} \times 10^6$ (Extended Data Fig. 1). A previous study¹⁰ suggested that the $\text{N}_2/^3\text{He}$ value of the Eifel source is $\sim 10^7$, slightly higher than estimates for the convective mantle (Extended Data Fig. 1). This is confirmed by our new $\text{N}_2/^3\text{He}$ and Δ_{30} data shown in Fig. 2 for two Eifel samples. Crustal contamination may not account for those signatures. We show below that crustal gases show $\text{N}_2/^{36}\text{Ar}$ ratios that are lower by one order of magnitude than the mantle. A crustal contribution therefore could not account for the high values observed in Eifel. We conclude that crustal contamination is unlikely to account for the nitrogen budget in the Eifel springs.

Mixing between mantle endmembers may account for the data. The European lithospheric mantle has been suggested to have a MORB-like $\delta^{15}\text{N}$ value on the basis of mineral spring $\delta^{15}\text{N}$ values⁵² without measurements of Δ_{30} . Mixing between a plume and the local lithospheric mantle could in principle account for the observed $\delta^{15}\text{N}$ of -1.4% but would leave the marginally high $\text{N}_2/^{36}\text{Ar}$ value derived for Eifel ($4.7_{-1.6}^{+0.8} \times 10^6$) unexplained: if plume sources were assigned a $\text{N}_2/^{36}\text{Ar}$ value of 10^6 or less, no mixing can successfully account for the data. For this mixing to be successful, the European lithospheric mantle must be assigned an anomalously high $\text{N}_2/^{36}\text{Ar}$ ratio. A mass balance shows that a $\text{N}_2/^{36}\text{Ar}$ value $>10^8$ is needed for any mixing curve to fit the Eifel datapoint. Such a value would be two orders of magnitude higher than the convective mantle and would be derived from either an -100 -fold enrichment in N or an -100 -fold depletion in ^{36}Ar from a precursor similar to the MORB mantle. It is unclear how a massive N enrichment could occur in the lithospheric mantle while preserving a MORB-like $\delta^{15}\text{N}$ value. Nitrogen and Ar have an undistinguishable solubility in silicate melts⁵³. Thus, melting and freezing processes bringing materials from the asthenosphere (with a $\delta^{15}\text{N}$ of -5%) to the lithosphere would not decouple N from Ar. Subduction-derived fluids could potentially increase the $\text{N}_2/^{36}\text{Ar}$ of the local lithospheric mantle but they are expected to have $\delta^{15}\text{N}$ value greater than -5% (ref. 8) and atmospheric $^{40}\text{Ar}/^{36}\text{Ar}$ values (refs. 54,55). This is not observed. Lastly, note that the need for a deep plume component is challenged by noble gas data. Although originally suggested to account for some Ne isotope data from Eifel xenoliths⁵⁶, such a deep plume component was ruled out⁵⁷ on samples from the same location. Some xenon isotopic data for Eifel free gas⁵⁸ also suggested the occurrence of a plume, but newer studies^{31,59} have not been able to reproduce the plume-like Xe isotope anomalies, obviating the need for any plume to account for Xe in European volcanic regions.

We suggest that Eifel gases reflect a mixing between the convective mantle and a recycled component with an $\text{N}_2/^{36}\text{Ar}$ of $\sim 10^7$ or higher, a $\text{N}_2/^3\text{He}$ of $\sim 10^{12}$ or higher and $\delta^{15}\text{N}$ of 1.5% (Extended Data Figs. 1, 6). The $\delta^{15}\text{N}$ of 1.5% is within the $\delta^{15}\text{N} = 2.8 \pm 1.2\%$ (1σ) for recycled oceanic crust based on alpine ophiolites¹³. The Eifel recycled crust component could be accounted for by the contribution of $<0.1\%$ sediment ($[\text{N}] = 400$ ppm; see below) to the convective mantle ($[\text{N}] = 0.3$ ppm, $\delta^{15}\text{N} = -5\%$)⁴. Note that the contribution of 3% recycled oceanic crust ($[\text{N}] = 6$ ppm)¹³ with a $\delta^{15}\text{N}$ of 1.5% to the convective mantle ($[\text{N}] = 0.3$ ppm, $\delta^{15}\text{N} = -5\%$)⁴ also fits the data. If $[\text{N}] = 0.6$ ppm is taken as characteristic of a devolatilized recycled crust, a mantle source containing 30% subducted material is needed to account for the Eifel data, in line with the typical 10 – 50%

estimated for recycled oceanic crust in the convective mantle⁶⁰. This idea is consistent with the marble cake mantle concept²³, where recycled pyroxenites are mixed with depleted lherzolites as a consequence of subduction. For MORBs, recycled oceanic crust contributions are generally 10% (refs. ^{23,60}), and $\delta^{15}\text{N}$ values remain unaffected by varying amounts of recycled components³. We suggest that in Eifel, the recycled component contribution is >10% and can impact the nitrogen budget. The marble cake concept also accounts for the mildly radiogenic helium dominating the mineral springs and the xenoliths in Eifel ($^3\text{He}/^4\text{He} = 5\text{--}6R_A$), as the occurrence of recycled pyroxenite tends to add ^4He to a resulting mantle source as a result of U and Th decay⁶¹. This decreases $^3\text{He}/^4\text{He}$ of a given mantle source from an asthenospheric ratio of $8R_A$ towards more radiogenic values^{61,62}.

The influence of crustal gases on Yellowstone samples and insights from Canadian craton nitrogen samples

Roughly half of the 13 gases from Yellowstone have $^3\text{He}/^4\text{He}$ ratios higher than the convective mantle value of $(8 \pm 1)R_A$ (ref. ⁴⁴), up to $14.7R_A$, similar to gases described in a previous study³⁰. Other gases show average radiogenic $^3\text{He}/^4\text{He}$ values of $(2.2 \pm 1.0)R_A$, which are low compared with the convective mantle value. This reflects the well-known contribution of radiogenic ^4He accumulated in the continental crust over 1 Gyr or more, within the underlying Archaean craton, released to the hydrothermal system by metamorphism induced by magmatic activity⁶³. The cratonic gases with radiogenic He also have radiogenic ^{40}Ar excesses and the possibility that N accompanies crustal ^4He requires evaluation. Yellowstone gas 'Yellowstone sample 2' has the highest $^3\text{He}/^4\text{He}$ value of the sample collection ($14.7R_A$; Supplementary Table 1). This value indicates that it is the sample with the lowest influence of crustal ^4He . This gas has nitrogen isotope systematics similar to other samples, which suggests that nitrogen is independent of contaminating crustal ^4He , as would be the case if crustal fluids were ^4He -rich but N-depleted. To constrain the amount of crustal nitrogen in Yellowstone samples, we make use of $\text{N}_2/^3\text{He}$ ratios. We show below that fluids from ancient crust are broadly similar to that underlying Yellowstone have $\text{N}_2/^3\text{He}$ values of $\sim 10^8$, far higher than mantle values observed at Yellowstone.

We report the composition of gases from the Kidd Creek mine (Timmins, Ontario, Canada) and the Nickel Rim mine (Sudbury, Ontario, Canada), both in the Superior Province of the Canadian Shield. These deep mines are located in the Archaean basement of the Canadian craton (2.6–2.7 Gyr old), consisting primarily of felsic, mafic, ultramafic and metasedimentary deposits⁶⁴. The Kidd Creek mine is situated within a volcanogenic massive sulfide deposit dated to ~ 2.7 Ga. The Sudbury mine is also located in Archaean basement underlying the Sudbury Igneous Complex formed by a massive impact event 1.85 Ga (see Warr et al.⁶⁴ and references therein). Gases that accumulated in fracture fluids over geologic time were recently investigated for noble gas isotopes^{64,65}. The chemical compositions of these gases (H_2 , O_2 , N_2 , Ar and He) were measured at the University of Toronto, and their N_2 isotope ratios were measured at UCLA.

For gases from Kidd Creek, we find N_2 concentrations around ~ 15 vol%, with Δ_{30} values between $1.1 \pm 0.4\%$ and $0.7 \pm 0.2\%$. For two gases composed of $\sim 50\%$ N_2 from the Sudbury mine, we find an average Δ_{30} of $0.5 \pm 0.2\%$ (2σ , $n = 2$). The nitrogen isotope data are consistent with the generation of crustal N_2 via metamorphism with no substantial ^{15}N excess, in agreement with thermodynamic predictions ($\Delta_{30} < 1\%$ at $T > 100$ °C). The data also demonstrate that sample collection was achieved with negligible atmospheric contamination. The average $\delta^{15}\text{N}$ of these gases is $+6.7 \pm 0.2\%$ (2σ , $n = 4$) at Kidd Creek and $+2.7 \pm 0.4\%$ (2s.d. , $n = 2$) at Sudbury. We suggest that these markedly positive values reflect metamorphism of the local crust, during which NH_4^+ -bearing silicates break down and release N_2 to the fracture fluids, possibly with kinetic isotopic fractionation favouring the release of ^{14}N over ^{15}N in the gas phase⁶⁶. Independently of a potential fractionation, the mine data are consistent with metamorphism forcing nitrogen devolatilization

to completion, liberating N_2 with $\delta^{15}\text{N}$ values similar to the local NH_4^+ -bearing rock precursor, as has been previously suggested for other sites on the Canadian and Fennoscandian cratons⁶⁷.

We measure between 3.6 and 4.8 vol% He in the Kidd Creek gases and between 24.1 and 27.7 vol% He in the Sudbury gases, similar to previous measurements^{35,68}. These gases were previously shown to have average $^3\text{He}/^4\text{He}$ ratios of $(0.022 \pm 0.001)R_A$ in the case of Kidd Creek and 0.019 ± 0.001 in the case of Sudbury^{64,65}. Errors are 1σ , see ref. ⁶⁴. These radiogenic excesses result from ^4He accumulation from crustal production over 0.5–1.0 Ga (ref. ⁶⁴). Taking the full dataset, we compute N_2/He , $\text{N}_2/^3\text{He}$ and $\text{N}_2/^{36}\text{Ar}$ ratios of 5.1 ± 0.7 , $1.8 (\pm 0.2) \times 10^8$ and $4.2 (\pm 0.1) \times 10^5$, respectively, for Kidd Creek gases. For Sudbury, we derive N_2/He , $\text{N}_2/^3\text{He}$ and $\text{N}_2/^{36}\text{Ar}$ similar to the gases observed at the Kidd Creek mine with values of 1.9 ± 0.1 , $0.7 (\pm 0.1) \times 10^8$ and $0.9 (\pm 0.3) \times 10^5$, respectively. Future studies will include additional cratonic locations, but, on the basis of these data, we suggest that continental crust has N_2/He , $\text{N}_2/^3\text{He}$ and $\text{N}_2/^{36}\text{Ar}$ ratios markedly distinct from the mantle values of 150, 1×10^6 and 2×10^6 , respectively (Fig. 3).

The derived $\text{N}_2/^{36}\text{Ar}$ ratios of the cratonic gases at Kidd Creek are marginally lower than mantle estimates, but have dramatically radiogenic $^{40}\text{Ar}/^{36}\text{Ar}$ ratios⁴⁰. In Fig. 3 we show the result of mixing between air and a Kidd Creek type gas with extremely high ^{40}Ar excesses ($^{40}\text{Ar}/^{36}\text{Ar}$ taken at 100,000; ref. ⁶⁴). The mixing fails to account for the Yellowstone data. We note, however, that lower $^{40}\text{Ar}/^{36}\text{Ar}$ values are observed in other cratonic gases, for example values of $\sim 5,000$ at Sudbury⁶⁴. The $\text{N}_2/^{36}\text{Ar}$ ratio there is $0.9 (\pm 0.3) \times 10^5$, similar to the low end of mantle reservoir estimates⁴. Thus, a mixing of air with Sudbury gas would generate mixing trends that could fortuitously fit plume data (with high $\text{N}_2/^{36}\text{Ar}$ and low $^{40}\text{Ar}/^{36}\text{Ar}$ values). In other words, the potential overlap in ranges of $\text{N}_2/^{36}\text{Ar}$ ratios of crustal and mantle gases prevent this approach from being used to identify and quantify the origin of N_2 and Ar in the Yellowstone samples.

The $\text{N}_2/^3\text{He}$ ratios of mantle gases are expected to be lower than those of the crust by two orders of magnitude, making this ratio a sensitive indicator of cratonic gas influences. The $\text{N}_2/^3\text{He}$ observed in the Yellowstone gases is clearly within the range of mantle values, well below both air and crustal values derived here. The $\text{N}_2/^3\text{He}$ values therefore can instead rule out any substantial crustal N_2 contributions in our Yellowstone gases. Mass balance shows that only 0.1% crustal contribution with a $^3\text{He}/^4\text{He}$ of $0.02R_A$ to 99.9% of a mantle gas (taken here to have $^3\text{He}/^4\text{He} = 16R_A$) overwhelms the ^4He content of the mixture, resulting in $^3\text{He}/^4\text{He}$ of roughly $2R_A$ and N_2/He ratios dropping from 150 to 10, similar to the observations in the ^4He -rich gases. Meanwhile, the $\text{N}_2/^3\text{He}$ ratio only increases from 1.0×10^6 to 1.2×10^6 . We thus conclude that on the basis of our low $\text{N}_2/^3\text{He}$ ratios, mantle nitrogen dominates the gases with crustal ^4He and we can neglect the influence of crustal N_2 .

Sedimentary nitrogen recycled in Yellowstone?

The Yellowstone plume is characterized by high $^3\text{He}/^4\text{He}$, suggesting the contribution of a relatively undegassed, primitive mantle source^{23,51}. We show that the plume has a $\text{N}_2/^3\text{He}$ ratio of $\sim 10^6$ (Fig. 2 and Extended Data Fig. 1) in agreement with a previous study³⁰. The Yellowstone data in Fig. 3 define an $\text{N}_2/^{36}\text{Ar}$ ratio of $1.6_{-0.4}^{+0.7} \times 10^6$ for the plume. This ^3He -rich plume source has $\text{N}_2/^3\text{He}$ and $\text{N}_2/^{36}\text{Ar}$ ratios indistinguishable from the convective mantle and a $\delta^{15}\text{N}$ value that is as high as that for nitrogen in descending slabs lithosphere (Extended Data Fig. 1). Nitrogen subduction could account for the data if descending plates of lithosphere with $\text{N}_2/^3\text{He}$ ratios of $\sim 10^{12}$ (ref. ³²) mix with a ^3He -rich mantle source that has an arbitrarily low $\text{N}_2/^3\text{He}$ ratio (≤ 2.10 ; see ref. ⁵ and Extended Data Fig. 6). The enriched, recycled components may be contained within the lithosphere (for example, as subduction fluids) if the lithosphere is assimilated into the plume⁶⁹. Alternatively, recycled components may be subducted oceanic crust, or sediments. In all cases, those scenarios of nitrogen addition are difficult to reconcile with the low $\text{N}_2/^3\text{He}$ ratio of Yellowstone, derived in Fig. 2.

Sediments carried down by the descending slabs of lithosphere contain much greater concentrations of nitrogen than mantle reservoirs, meaning that recycled sediments can, in principle, easily affect the resulting nitrogen budget of mantle sources. These are usually invoked to account for positive $\delta^{15}\text{N}$ values in plumes^{4,6}. The exact median nitrogen concentration in sediments remains unknown, but Busigny et al.¹⁴ showed that sediments have a well-constrained K/N ratio of 14. Using the global modern sediment K_2O estimate of 2.04 wt% derived by Plank and Langmuir⁷⁰, we calculate that global sediments in the present day contain roughly 400 ppm N. The nitrogen concentration of mantle reservoirs (the ^3He -source of Yellowstone, or even the convective mantle) is, however, extremely poorly known. The convective mantle is assumed to have 0.3 ppm nitrogen⁴ but considerably higher estimates exist¹. One may assume that the high $^3\text{He}/^4\text{He}$ of the Yellowstone mantle source reflects a relatively undegassed mantle source²³. If so, it may contain a concentration of ^3He that is 100× higher than the convective mantle²³. If the Yellowstone source is required to have an $\text{N}_2/^3\text{He}$ ratio lower than the convective mantle by one order of magnitude to obtain a successful mixing scenario (Extended Data Fig. 6), the nitrogen concentration of the ^3He -rich source would be only 10× higher than the convective mantle, that is, 3 ppm (see other plume estimates at 3 ppm N in ref. ⁴). Adding sediments to this source would yield the observed $\delta^{15}\text{N}$, $\text{N}_2/^{36}\text{Ar}$ and $\text{N}_2/^3\text{He}$ ratios if sediments contributed 10% to the Yellowstone mantle source; Yellowstone volatiles would result from 90% ^3He -rich primordial mantle and 10% recycled sediment. The source would have a total concentration of roughly 30 ppm N. Lower nitrogen concentrations in the ^3He -rich source tend to lower the required sediment contribution. If the nitrogen concentration in the ^3He -source is arbitrarily taken to be 0.3 ppm, the Yellowstone data can be satisfied by the addition of just 1% sediment. Conversely, if the nitrogen concentration is >3 ppm (ref. ¹), the required sediment contribution would be greater than 10%. The addition of such large amounts of sediments would have resulted in obvious trace element and radiogenic isotopic signatures of the contaminated plumes (for example, cerium or niobium anomalies and high time-integrated Rb/Sr ratios, see Class et al.⁷¹, Eisele et al.⁷² or Jackson et al.⁷³ and references therein). In fact, only the few plumes of enriched-mantle type (for example, Pitcairn, Samoa, Society) are regarded as exhibiting discernible sedimentary contributions⁷³, typically up to -1%, but with exceptions. Society could host -1–5% sediment⁷⁴. Here mantle-derived $\delta^{15}\text{N}$ is high, suggestive of sedimentary input⁴, and the gases have high $\text{N}_2/^3\text{He}$ ratios, ranging up to $\sim 10^9$, three orders of magnitude greater than the convective mantle¹¹. The scenario of sedimentary nitrogen is internally consistent with these results and seems unavoidable to account for those data, but no such sedimentary contributions are known in the source of Yellowstone^{69,75}.

$\text{N}_2/^{36}\text{Ar}$ ratios of volcanic endmembers in gases

Historically, the $^{40}\text{Ar}/^{36}\text{Ar}$ ratios of mantle endmembers have been deduced using relationships between $^{40}\text{Ar}/^{36}\text{Ar}$ and $^{20}\text{Ne}/^{22}\text{Ne}$ ratios in volcanic rocks and gases^{44,51,76}. For Eifel, the extrapolated $^{40}\text{Ar}/^{36}\text{Ar}$ value of the mantle was calculated to be 39, 400 $_{-15,200}^{+2,900}$ in ref. ³¹. This in turn can be used to fit the data in Fig. 3 with an $\text{N}_2/^{36}\text{Ar}$ ratio of $4.7_{-1.6}^{+0.8} \times 10^6$. For Yellowstone, further work is needed to derive an $^{40}\text{Ar}/^{36}\text{Ar}$ isotope ratio for the plume endmember. Using a lower limit $^{40}\text{Ar}/^{36}\text{Ar}$ ratio of 5,000 (similar to the Kola plume) yields an $\text{N}_2/^{36}\text{Ar}$ ratio of 1.1×10^6 (Fig. 3). Using an upper limit $^{40}\text{Ar}/^{36}\text{Ar}$ isotope ratio of 13,000, similar to Iceland, yields an $\text{N}_2/^{36}\text{Ar}$ ratio of 2.4×10^6 . We use the $\text{N}_2/^{36}\text{Ar}$ ratio of 1.4×10^6 obtained at an intermediate $^{40}\text{Ar}/^{36}\text{Ar}$ ratio of 10,000. Thus, using various $^{40}\text{Ar}/^{36}\text{Ar}$ values for mantle plumes does not change our conclusion that $\text{N}_2/^{36}\text{Ar}$ for the Yellowstone mantle plume is indistinguishable from the convective mantle.

Two-box model of the nitrogen exchange between the convective mantle and surface

We consider the time evolution of the amount of nitrogen in two global reservoirs, the convective mantle and the surface, where the latter is

dominated by N_2 in air. Similar exercises have been done to document the evolution of terrestrial xenon⁷⁷. We describe the slow, tectonically controlled geological nitrogen cycle. In this work, the convective mantle is the reservoir sampled by MORBs, and is considered to incorporate the upper mantle and a large fraction of the lower mantle (see ref. ⁵ and references therein). Through outgassing and subduction, this is the reservoir that is susceptible to reaching a steady state with the surface. Plume sources are not considered part of the convective mantle, but may combine primordial and recycled noble gas signatures⁵¹. On the surface, biogeochemical cycling of nitrogen between air, organic matter and sediments leaves ~ 70 – 90% of the nitrogen in air⁷⁸. Nitrogen in organic matter and sediments has an average $\delta^{15}\text{N}$ value of 3‰ through deep time, with the exception of a few excursions^{24,79}. On this basis, we estimate that the average $\delta^{15}\text{N}$ value for the surface is 0.5‰. Slightly different estimates do not change the results of our models. Note that biological activity quantitatively cycles nitrogen over timescales of a few million years only⁷⁸. Biological cycles are thus negligible in the context of this study, beyond providing a means for sequestering nitrogen from air into sediments.

Nitrogen leaves the surface by subduction principally as NH_4^+ in clay minerals, feldspars and micas⁷⁸. Nitrogen is returned to the surface by active volcanism. The ordinary differential equations representing the time evolution of the amount of nitrogen in the mantle and at the surface are:

$$\begin{aligned} \frac{dn_{\text{N}}^{\text{Mantle}}}{dt} &= k_{\text{sub}} n_{\text{N}}^{\text{Surface}} - k_{\text{vol}} n_{\text{N}}^{\text{Mantle}} \\ \frac{dn_{\text{N}}^{\text{Surface}}}{dt} &= -k_{\text{sub}} n_{\text{N}}^{\text{Surface}} + k_{\text{vol}} n_{\text{N}}^{\text{Mantle}} \end{aligned} \quad (2)$$

where t is time and n_{N}^i refers to the quantity of N (for example, moles of N) in reservoir i . The solution of equation (2) for the time-dependent abundance of N in the mantle is

$$\begin{aligned} n_{\text{N}}(t)^{\text{Mantle}} &= \left(\frac{k_{\text{vol}}}{k_{\text{vol}} + k_{\text{sub}}} n_{0,\text{N}}^{\text{Mantle}} - \frac{k_{\text{sub}}}{k_{\text{vol}} + k_{\text{sub}}} n_{0,\text{N}}^{\text{Surface}} \right) \\ &\quad \exp[-(k_{\text{vol}} + k_{\text{sub}})t] + \frac{k_{\text{sub}}}{k_{\text{vol}} + k_{\text{sub}}} (n_{0,\text{N}}^{\text{Mantle}} + n_{0,\text{N}}^{\text{Surface}}) \end{aligned} \quad (3)$$

where i subscript 0 refers to the initial values. The second term on the right is the solution at steady state (for example, when $t \rightarrow \infty$). The isotopic effects in the mantle are obtained by evaluating equation (3) for both ^{14}N and ^{15}N and taking the ratio of the results. In the case of ^{15}N , the rate constant for subduction, k_{sub} , is multiplied by the $^{15}\text{N}/^{14}\text{N}$ isotope fractionation factor associated with subduction ($\alpha_{\text{sub}} = (^{15}\text{N}/^{14}\text{N})_{\text{sub}} / (^{15}\text{N}/^{14}\text{N})_{\text{Surface}}$). We assume no fractionation between mantle nitrogen and that delivered to the surface by volcanism. Equation (3) shows explicitly that when $k_{\text{sub}} \ll k_{\text{vol}}$, a steady state leads to no nitrogen in the mantle. Conversely, when $k_{\text{sub}} \gg k_{\text{vol}}$, the mantle contains virtually all of Earth's nitrogen. The utility of equation (3) is for those circumstances in between.

We explored a wide variety of time-dependent models using present-day fluxes from previous work¹³ where the free parameters are the starting $\delta^{15}\text{N}$ and N quantities for the surface and mantle. We ran the models with the additional constraint that the surface must end up with 3.2×10^{20} mol N and an average $\delta^{15}\text{N}$ of 0.5‰ (ref. ⁴) at the present day. The models were evaluated on the basis of whether or not they could evolve to yield 0.3 ± 0.3 ppm N in the mantle after 4.5 Gyr. In all cases, the models approach isotopic steady state, leaving the mantle isotopically heavier than present-day air. Applying current fluxes through deep time also predicts a threefold decrease in nitrogen concentration in the surface reservoir over time. This has been invoked⁸⁰ in earlier work, but is in conflict with data from ancient fluid inclusions^{33,81,82} and sediments^{24,79}. The model results therefore imply that modern nitrogen subduction and degassing fluxes are not relevant to deep

time. Note that these calculations were performed assuming a mantle nitrogen concentration of 0.3 ppm (ref. ⁴). In this case, the mantle and surface reservoirs contain roughly the same quantities of nitrogen, that is, 10^{20} mol N. If the mantle is assumed to presently contain 30 ppm (ref. ¹), this reservoir dominates Earth's nitrogen budget, comprising >99% of the mantle–surface nitrogen system. In this case, no exchange scenario can substantially modify the mantle $\delta^{15}\text{N}$ without a 100-fold consequence to the surface nitrogen abundance and our conclusion that mantle nitrogen is mostly primordial would be reinforced.

We explored the possibility of evolving fluxes over geological time. To solve the differential equation (2) with varying fluxes, and therefore varying rate constants k_{vol} and k_{sub} , the model was adjusted at each time step, with each previous step comprising the initial condition for the step that follows. In this way, by iteratively solving the differential equations at each time step ($\Delta t = 200$ Myr), the evolution of nitrogen abundances and isotope ratios were traced through time (Extended Data Fig. 7). We verified that our solutions are invariant with respect to smaller time step sizes. In this context, we note again that since the characteristic timescale for biological nitrogen cycling is ~20 Myr, biogeochemical nitrogen exchanges within the surface reservoir cannot substantially alter the results described here. We considered variable rates of subduction and volcanism over time. Any model with subduction fluxes larger than volcanic outgassing fluxes over most of the Earth's history fails to account for present-day observations, regardless of the initial $\delta^{15}\text{N}$ values of the mantle and surface; eventually, a steady state is achieved where $\delta^{15}\text{N}_{\text{Mantle}} > \delta^{15}\text{N}_{\text{Surface}}$. The only models that satisfy the present-day observations in terms of relative quantities and isotope ratios of nitrogen, without requiring dramatic secular evolution in the surface abundances of nitrogen, require subduction fluxes considerably lower than volcanic outgassing fluxes over most of the Earth's history. For example, we computed a scenario where subduction fluxes are one to two orders of magnitude lower than the present day throughout the Archaean and the Proterozoic. This was combined with volcanic fluxes steadily decreasing through time, with a starting point one to two orders of magnitude greater than the present-day fluxes. This is consistent with generally higher degassing fluxes early in Earth's history inferred from noble gas data^{83,84}. This scenario would require the net degassing of $\sim 3 \times 10^{19}$ mol N_2 over Earth's history, which represents ~20% of the N_2 abundance in the modern-day atmosphere. This model can return present-day nitrogen isotope ratios and concentrations in the two reservoirs without requiring dramatic secular evolution of nitrogen abundances and $^{15}\text{N}/^{14}\text{N}$ in the reservoirs (Fig. 4).

The idea of low subduction fluxes of nitrogen in the past requires further investigation. It may require extremely low nitrogen concentrations in sediments older than the Phanerozoic Eon, as observed in previous studies for Archaean sediments⁸⁵. It may also be consistent with the prevalence of hot subduction zones in the past, resulting in near-quantitative nitrogen losses from the subducting slab. In these cases, nitrogen is returned to air via arc outgassing, as observed in some present-day arcs⁸.

Data availability

Nitrogen isotopologue and noble gas data are archived on EarthChem at <https://doi.org/10.1594/IEDA/111481>. Source data for Figs. 1–3 are provided with the paper.

34. Giggenbach, W. & Goguel, R. *Collection and Analysis of Geothermal and Volcanic Water and Gas Discharges* Report No. CD 2401 (Chemistry Division, DSIR, 1989).
35. Sherwood Lollar, B., Westgate, T., Ward, J., Slater, G. & Lacrampe-Couloume, G. Abiogenic formation of alkanes in the Earth's crust as a minor source for global hydrocarbon reservoirs. *Nature* **416**, 522–524 (2002).
36. Young, E. D., Rumble, D., III, Freedman, P. & Mills, M. A large-radius high-mass-resolution multiple-collector isotope ratio mass spectrometer for analysis of rare isotopologues of O_2 , N_2 , CH_4 and other gases. *Int. J. Mass Spectrom.* **401**, 1–10 (2016).
37. Barry, P. et al. Noble gases solubility models of hydrocarbon charge mechanism in the Sleipner Vest gas field. *Geochim. Cosmochim. Acta* **194**, 291–309 (2016).

38. Fischer, T. P. et al. Temporal variations in fumarole gas chemistry at Poás volcano, Costa Rica. *J. Volcanol. Geotherm. Res.* **294**, 56–70 (2015).
39. Rizzo, A. L. et al. Kolombo submarine volcano (Greece): an active window into the Aegean subduction system. *Sci. Rep.* **6**, 28013 (2016).
40. Ward, J. A. et al. Microbial hydrocarbon gases in the Witwatersrand Basin, South Africa: implications for the deep biosphere. *Geochim. Cosmochim. Acta* **68**, 3239–3250 (2004).
41. Sherwood Lollar, B. et al. Unravelling abiogenic and biogenic sources of methane in the Earth's deep subsurface. *Chem. Geol.* **226**, 328–339 (2006).
42. Sano, Y. et al. Origin of methane-rich natural gas at the West Pacific convergent plate boundary. *Sci. Rep.* **7**, 15646 (2017).
43. Sarda, P. & Graham, D. Mid-ocean ridge popping rocks: implications for degassing at ridge crests. *Earth Planet. Sci. Lett.* **97**, 268–289 (1990).
44. Moreira, M., Kunz, J. & Allegre, C. Rare gas systematics in popping rock: isotopic and elemental compositions in the upper mantle. *Science* **279**, 1178–1181 (1998).
45. Middleton, J. L., Langmuir, C. H., Mukhopadhyay, S., McManus, J. F. & Mitrovica, J. X. Hydrothermal iron flux variability following rapid sea level changes. *Geophys. Res. Lett.* **43**, 3848–3856 (2016).
46. Jones, M. et al. New constraints on mantle carbon from Mid-Atlantic Ridge popping rocks. *Earth Planet. Sci. Lett.* **511**, 67–75 (2019).
47. Péron, S. et al. Noble gas systematics in new popping rocks from the Mid-Atlantic Ridge (14° N): evidence for small-scale upper mantle heterogeneities. *Earth Planet. Sci. Lett.* **519**, 70–82 (2019).
48. Cartigny, P., Pineau, F., Aubaud, C. & Javoy, M. Towards a consistent mantle carbon flux estimate: Insights from volatile systematics ($\text{H}_2\text{O}/\text{Ce}$, δD , CO_2/Nb) in the North Atlantic mantle (14°N and 34°N). *Earth Planet. Sci. Lett.* **265**, 672–685 (2008).
49. Cartigny, P., Jendrzejewski, N., Pineau, F., Petit, E. & Javoy, M. Volatile (C, N, Ar) variability in MORB and the respective roles of mantle source heterogeneity and degassing: the case of the Southwest Indian Ridge. *Earth Planet. Sci. Lett.* **194**, 241–257 (2001).
50. Füre, E. et al. Apparent decoupling of the He and Ne isotope systematics of the Icelandic mantle: the role of He depletion, melt mixing, degassing fractionation and air interaction. *Geochim. Cosmochim. Acta* **74**, 3307–3332 (2010).
51. Mukhopadhyay, S. Early differentiation and volatile accretion recorded in deep-mantle neon and xenon. *Nature* **486**, 101–104 (2012).
52. Bräuer, K., Kämpf, H., Niedermann, S., Strauch, G. & Weise, S. M. Evidence for a nitrogen flux directly derived from the European subcontinental mantle in the Western Eger Rift, central Europe. *Geochim. Cosmochim. Acta* **68**, 4935–4947 (2004).
53. Libourel, G., Marty, B. & Humbert, F. Nitrogen solubility in basaltic melt. Part I. effect of oxygen fugacity. *Geochim. Cosmochim. Acta* **67**, 4123–4135 (2003).
54. Broadley, M. W., Ballentine, C. J., Chavrit, D., Dallai, L. & Burgess, R. Sedimentary halogens and noble gases within Western Antarctic xenoliths: implications of extensive volatile recycling to the sub continental lithospheric mantle. *Geochim. Cosmochim. Acta* **176**, 139–156 (2016).
55. Matsumoto, T., Chen, Y. & Matsuda, J.-i. Concomitant occurrence of primordial and recycled noble gases in the Earth's mantle. *Earth Planet. Sci. Lett.* **185**, 35–47 (2001).
56. Buikin, A. et al. Noble gas isotopes suggest deep mantle plume source of late Cenozoic mafic alkaline volcanism in Europe. *Earth Planet. Sci. Lett.* **230**, 143–162 (2005).
57. Gautheron, C., Moreira, M. & Allègre, C. He, Ne and Ar composition of the European lithospheric mantle. *Chem. Geol.* **217**, 97–112 (2005).
58. Caracausi, A., Avicé, G., Burnard, P. G., Füre, E. & Marty, B. Chondritic xenon in the Earth's mantle. *Nature* **533**, 82–85 (2016).
59. Moreira, M., Rouchon, V., Muller, E. & Noirez, S. The xenon isotopic signature of the mantle beneath Massif Central. *Geochem. Perspect. Lett.* **6**, 28–32 (2018).
60. Sobolev, A. V. et al. The amount of recycled crust in sources of mantle-derived melts. *Science* **316**, 412–417 (2007).
61. Moreira, M. A., Dosso, L. & Ondréas, H. Helium isotopes on the Pacific-Antarctic ridge (52.5°–41.5° S). *Geophys. Res. Lett.* **35**, L10306 (2008).
62. Day, J. M. & Hilton, D. R. Origin of $^3\text{He}/^4\text{He}$ ratios in HIMU-type basalts constrained from Canary Island lavas. *Earth Planet. Sci. Lett.* **305**, 226–234 (2011).
63. Lowenstern, J. B., Evans, W. C., Bergfeld, D. & Hunt, A. G. Prodigious degassing of a billion years of accumulated radiogenic helium at Yellowstone. *Nature* **506**, 355–358 (2014).
64. Warr, O. et al. Tracing ancient hydrogeological fracture network age and compartmentalisation using noble gases. *Geochim. Cosmochim. Acta* **222**, 340–362 (2018).
65. Holland, G. et al. Deep fracture fluids isolated in the crust since the Precambrian era. *Nature* **497**, 357–360 (2013).
66. Li, L., Cartigny, P. & Ader, M. Kinetic nitrogen isotope fractionation associated with thermal decomposition of NH_3 : experimental results and potential applications to trace the origin of N_2 in natural gas and hydrothermal systems. *Geochim. Cosmochim. Acta* **73**, 6282–6297 (2009).
67. Sherwood Lollar, B. et al. Evidence for bacterially generated hydrocarbon gas in Canadian Shield and Fennoscandian Shield rocks. *Geochim. Cosmochim. Acta* **57**, 5073–5085 (1993).
68. Sherwood Lollar, B. et al. Abiogenic methanogenesis in crystalline rocks. *Geochim. Cosmochim. Acta* **57**, 5087–5097 (1993).
69. Jean, M. M., Hanan, B. B. & Shervais, J. W. Yellowstone hotspot–continental lithosphere interaction. *Earth Planet. Sci. Lett.* **389**, 119–131 (2014).
70. Plank, T. & Langmuir, C. H. The chemical composition of subducting sediment and its consequences for the crust and mantle. *Chem. Geol.* **145**, 325–394 (1998).
71. Class, C. & le Roex, A. P. Ce anomalies in Gough Island lavas—trace element characteristics of a recycled sediment component. *Earth Planet. Sci. Lett.* **265**, 475–486 (2008).
72. Eisele, J. et al. The role of sediment recycling in EM-1 inferred from Os, Pb, Hf, Nd, Sr isotope and trace element systematics of the Pitcairn hotspot. *Earth Planet. Sci. Lett.* **196**, 197–212 (2002).
73. Jackson, M. G. et al. The return of subducted continental crust in Samoan lavas. *Nature* **448**, 684–687 (2007).

74. Devey, C. W. et al. Active submarine volcanism on the Society hotspot swell (West Pacific): a geochemical study. *J. Geophys. Res. Solid Earth* **95**, 5049–5066 (1990).
75. Dodson, A., Kennedy, B. M. & DePaolo, D. J. Helium and neon isotopes in the Imnaha Basalt, Columbia River Basalt Group: evidence for a Yellowstone plume source. *Earth Planet. Sci. Lett.* **150**, 443–451 (1997).
76. Parai, R. & Mukhopadhyay, S. How large is the subducted water flux? New constraints on mantle degassing rates. *Earth Planet. Sci. Lett.* **317–318**, 396–406 (2012).
77. Parai, R. & Mukhopadhyay, S. Xenon isotopic constraints on the history of volatile recycling into the mantle. *Nature* **560**, 223–227 (2018); publisher correction 563, E28 (2018).
78. Johnson, B. & Goldblatt, C. The nitrogen budget of Earth. *Earth Sci. Rev.* **148**, 150–173 (2015); corrigendum 165, 377–378 (2017)
79. Ader, M. et al. Interpretation of the nitrogen isotopic composition of Precambrian sedimentary rocks: assumptions and perspectives. *Chem. Geol.* **429**, 93–110 (2016).
80. Goldblatt, C. et al. Nitrogen-enhanced greenhouse warming on early Earth. *Nat. Geosci.* **2**, 891–896 (2009).
81. Nishizawa, M., Sano, Y., Ueno, Y. & Maruyama, S. Speciation and isotope ratios of nitrogen in fluid inclusions from seafloor hydrothermal deposits at ~3.5 Ga. *Earth Planet. Sci. Lett.* **254**, 332–344 (2007).
82. Marty, B., Zimmermann, L., Pujol, M., Burgess, R. & Philippot, P. Nitrogen isotopic composition and density of the Archean atmosphere. *Science* **342**, 101–104 (2013).
83. Allègre, C. J., Staudacher, T. & Sarda, P. Rare gas systematics: formation of the atmosphere, evolution and structure of the Earth's mantle. *Earth Planet. Sci. Lett.* **81**, 127–150 (1987).
84. Avice, G., Marty, B. & Burgess, R. The origin and degassing history of the Earth's atmosphere revealed by Archean xenon. *Nat. Commun.* **8**, 15455 (2017).
85. Pinti, D. L., Hashizume, K. & Matsuda, J.-i. Nitrogen and argon signatures in 3.8 to 2.8 Ga metasediments: clues on the chemical state of the Archean ocean and the deep biosphere. *Geochim. Cosmochim. Acta* **65**, 2301–2315 (2001).
86. Marty, B. & Humbert, F. Nitrogen and argon isotopes in oceanic basalts. *Earth Planet. Sci. Lett.* **152**, 101–112 (1997).
87. Li, L. & Bebout, G. E. Carbon and nitrogen geochemistry of sediments in the Central American convergent margin: insights regarding subduction input fluxes, diagenesis, and paleoproductivity. *J. Geophys. Res. Solid Earth* **110**, B11202 (2005).
88. Schultz, L. & Franke, L. Helium, neon, and argon in meteorites: a data collection. *Meteorit. Planet. Sci.* **39**, 1889–1890 (2004).
89. Kerridge, J. F. Carbon, hydrogen, and nitrogen in carbonaceous chondrites: abundances and isotopic compositions in bulk samples. *Geochim. Cosmochim. Acta* **49**, 1707–1714 (1985).
90. Marty, B. et al. Origins of volatile elements (H, C, N, noble gases) on Earth and Mars in light of recent results from the ROSETTA cometary mission. *Earth Planet. Sci. Lett.* **441**, 91–102 (2016).

Acknowledgements This study was supported by the Deep Carbon Observatory through Sloan Foundation grant numbers G-2018-11346 and G-2017-9815 to E.D.Y. The Deep Carbon Observatory also supported field trips via grant numbers G-2016-7206 and G-2017-9696 to P. H.B. We thank S. Mukhopadhyay for providing a sample of popping rock; K. Farley for lending equipment; and J. Dottin, M. Bonifacie, V. Busigny, P. Cartigny and A. Shahar for helpful discussions.

Author contributions E.D.Y. designed the study. J.L. made the nitrogen isotopologue measurements of all mantle-derived samples and most cratonic samples, interpreted the data and wrote the manuscript with feedback from E.D.Y. E.D.Y. and J.L. constructed the box models. I.E.K. made nitrogen isotopologue measurements of some of the cratonic samples. P.H.B., D.V.B., M.W.B., T.P.F. and A.C. measured noble gas abundances and isotope ratios in mantle-derived samples. O.W. and T.G. measured major element chemistry in cratonic gases. P.H.B., D.V.B., M.W.B., T.P.F. and B.M. conducted field trips and sample collection in Yellowstone, USA. D.V.B., M.W.B. and B.M. conducted a field trip and sample collection in Eifel, Germany. P.H.B., A.S. and S.A.H. conducted a field trip and sample collection in Iceland. B.M. and T.P.F. conducted a field trip and sample collection in East Africa. T.P.F. conducted a field trip and sample collection in Hawaii. B.S.L., O.W. and T.G. conducted multiple field trips and sample collections in the Kidd Creek and Sudbury mines, Canada. G.A. assisted in acquiring data for popping rocks. M.D.K. contributed popping rock samples. All authors contributed to the final manuscript preparation.

Competing interests The authors declare no competing interests.

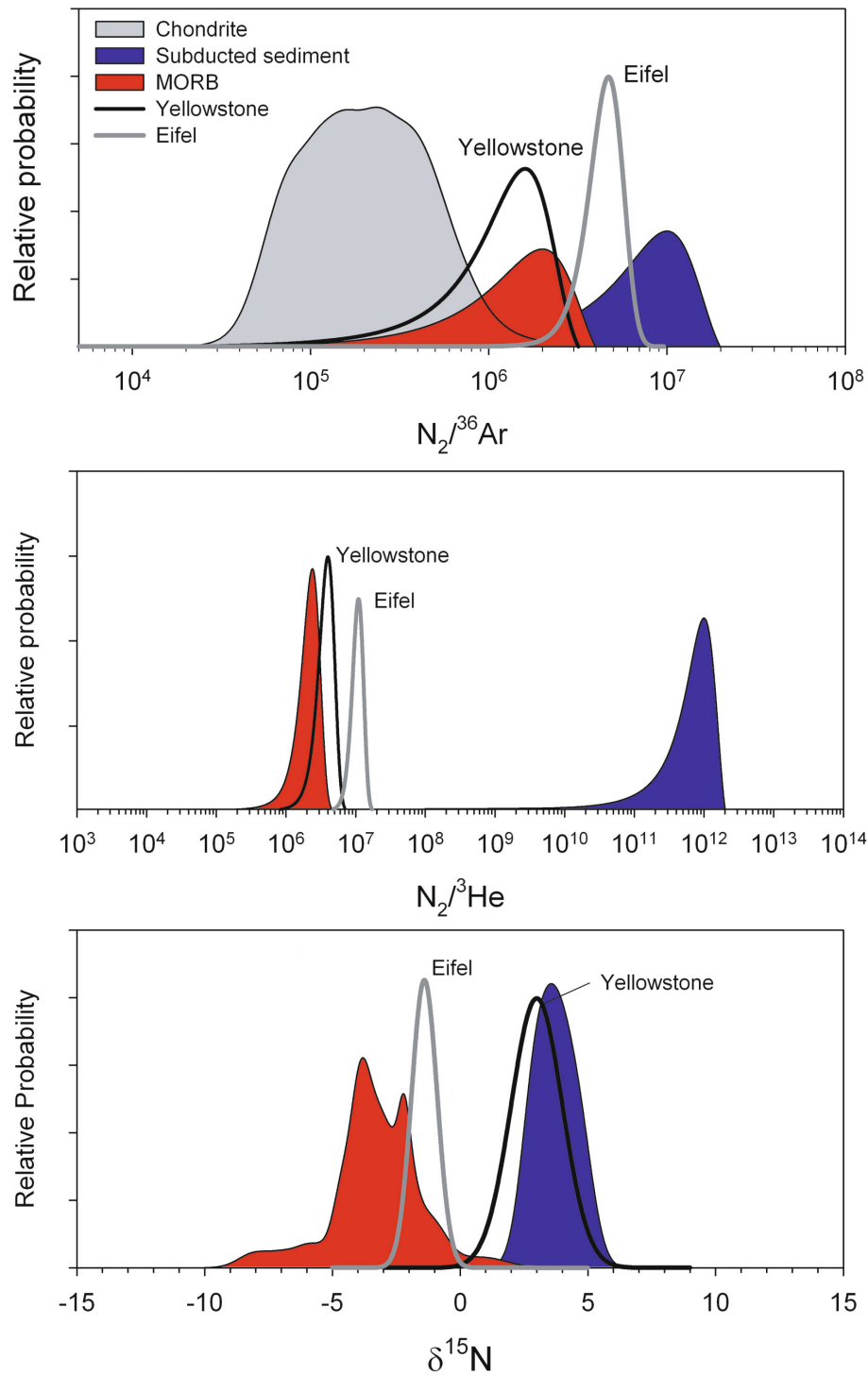
Additional information

Supplementary information is available for this paper at <https://doi.org/10.1038/s41586-020-2173-4>.

Correspondence and requests for materials should be addressed to J.L. or E.D.Y.

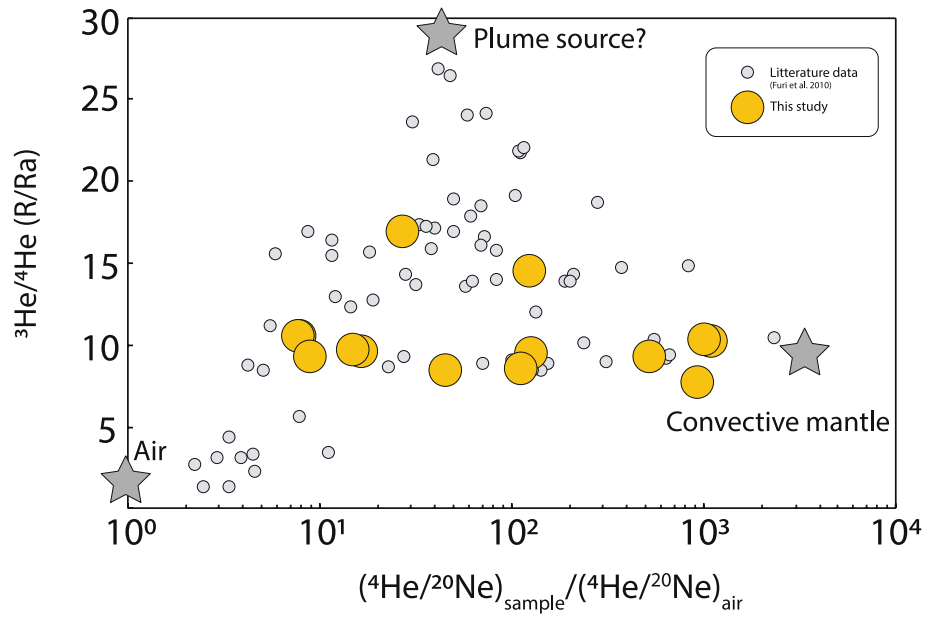
Peer review information *Nature* thanks Rita Parai and Yuji Sano for their contribution to the peer review of this work.

Reprints and permissions information is available at <http://www.nature.com/reprints>.



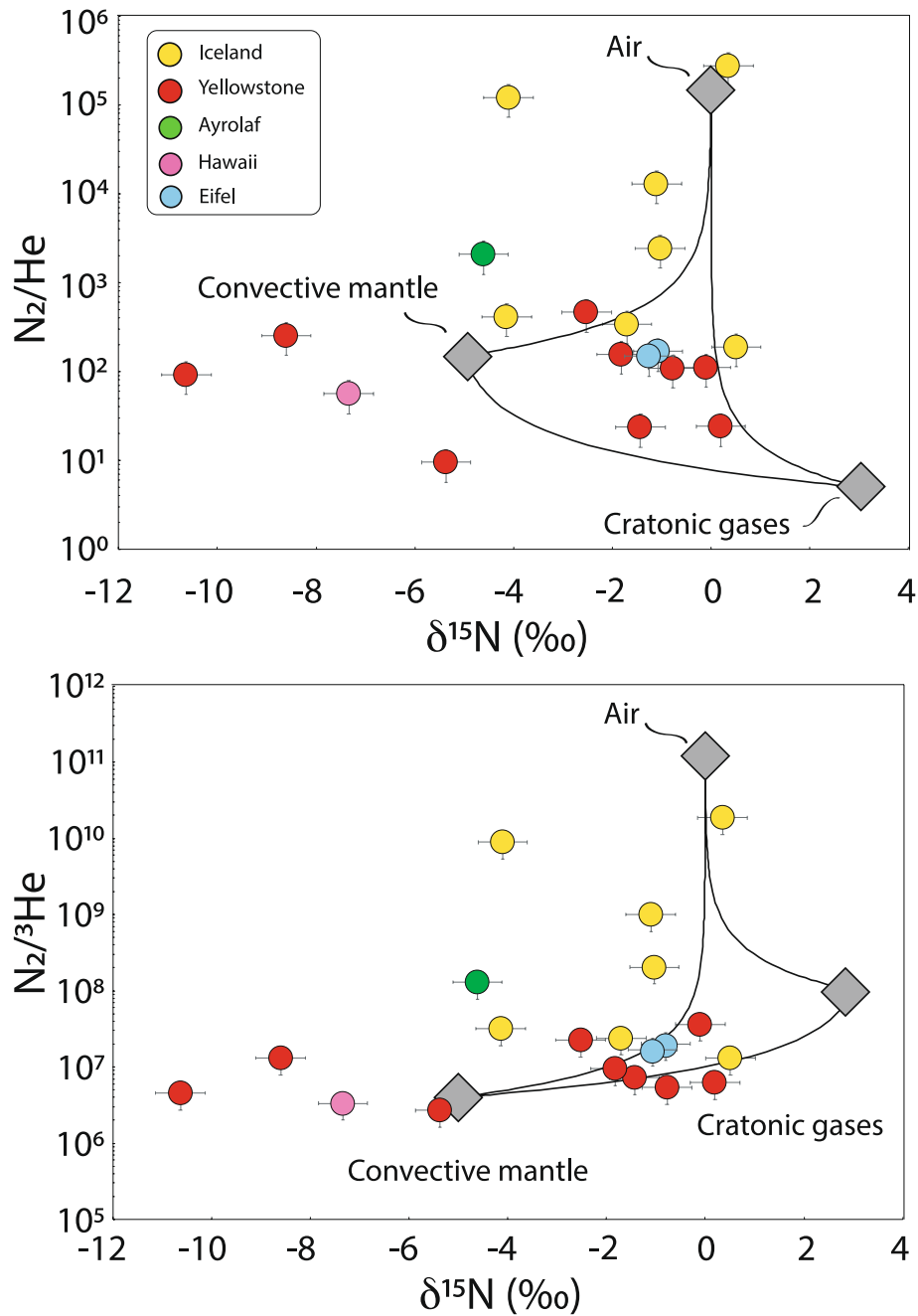
Extended Data Fig. 1 | Probability density plots for $N_2/^{36}Ar$, $N_2/^3He$ and $\delta^{15}N$ based on literature data and our study. The relative probabilities are scaled so that each probability is visible on the same plot. The probability densities for $\delta^{15}N$ are taken from the mean and standard deviation of the reported measured values in the cases of Yellowstone and Eifel. The $\delta^{15}N$ MORB^{3,4,9,86} and metasediment^{12,14,15,87} data were compiled from the literature. The probability densities for molecular ratios were calculated by taking the ratios of Monte Carlo draws for numerator and denominator and propagating nominal 20% errors assigned to each molecular concentration. Literature data for chondritic

$N_2/^{36}Ar$ were obtained using N and ^{36}Ar concentrations in individual chondrites^{19,88,89}. The dataset includes all major types of carbonaceous, enstatite and ordinary chondrites. No systematic difference could be observed between chondrite groups. Using this global dataset, we find that chondritic estimates used earlier^{3,90} for $N_2/^{36}Ar$ cannot be replicated. $N_2/^{36}Ar$ and $N_2/^3He$ estimates for metasediments are from Sano et al.³², assuming a normal distribution for the uncertainties. The convective mantle $N_2/^3He$ and $N_2/^{36}Ar$ data are from ref. ¹¹ and references cited in Extended Data Fig. 5.



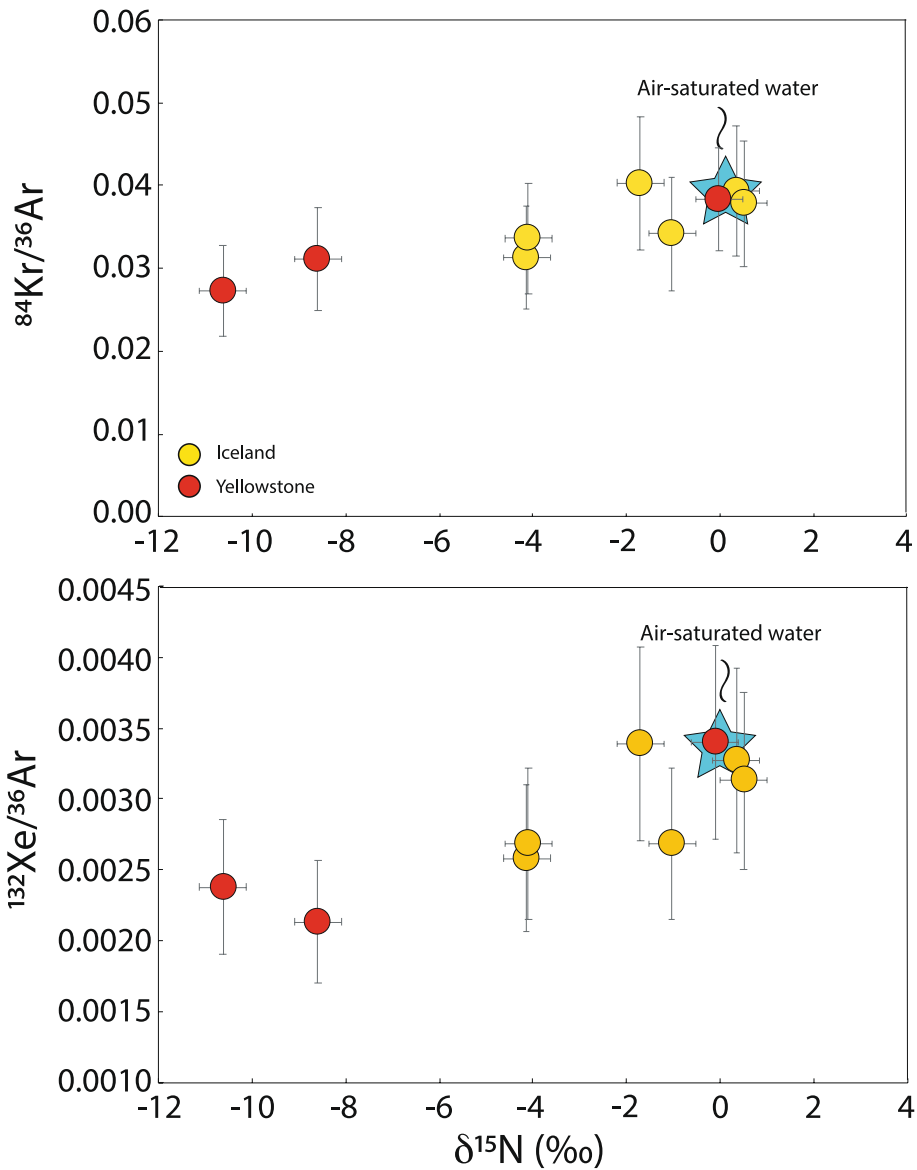
Extended Data Fig. 2 | $^3\text{He}/^4\text{He}$ of Icelandic gases plotted against their $^4\text{He}/^{20}\text{Ne}$ ratios normalized to air. Literature data⁵⁰ illustrate a three-component mixing with air, the convective mantle and the plume mantle. The convective mantle endmember is characterized by $^3\text{He}/^4\text{He}$ of $\sim 8 R_A$ and a

relatively high $^4\text{He}/^{20}\text{Ne}$ relative to air⁴⁴. The plume component is characterized by primordial $^3\text{He}/^4\text{He}$ values of up to $\sim 30 R_A$ and a $^4\text{He}/^{20}\text{Ne}$ value lower than the convective mantle^{50,51}. On this plot, our 11 samples have compositions with clear contributions from the three endmembers.



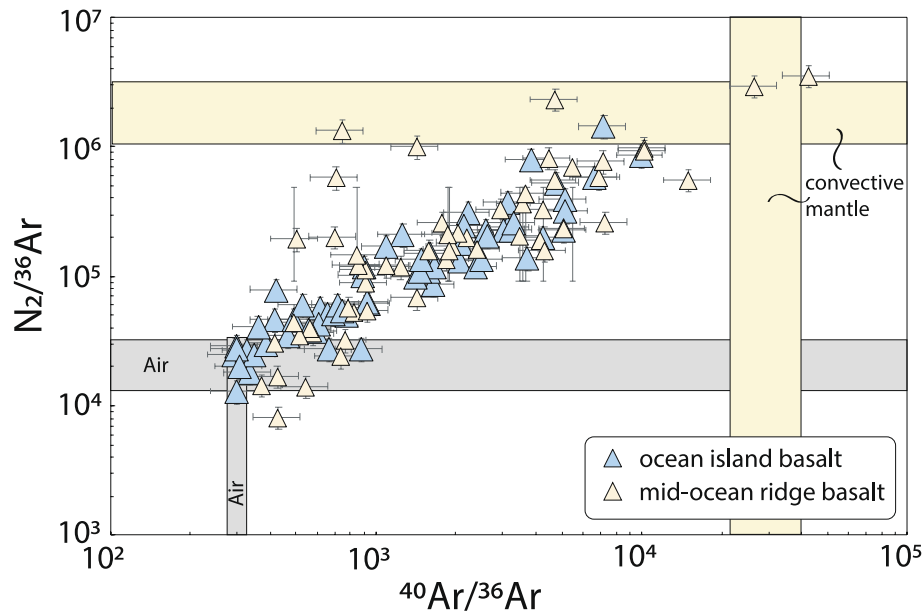
Extended Data Fig. 3 | N_2/He and $\text{N}_2/{}^3\text{He}$ ratios versus $\delta^{15}\text{N}$ in gases from Iceland, Yellowstone, Ayrolaf, Eifel and Hawaii. Top, values for N_2/He versus $\delta^{15}\text{N}$ for air, the convective mantle and cratonic gases compared with the samples from this study are shown. This is a similar plot to that in Fischer et al.⁸ except that cratonic gases are shown for the first time, to our knowledge. The extremely low N_2/He ratio for cratonic gases derived here results from substantial accumulation of ${}^4\text{He}$ over geological times. See the Supplementary Discussion for definitions of the cratonic gases based on samples from the Canadian Shield (data in Supplementary Table 2). In this space, data are usually interpreted as representing ternary mixtures. However, this plot fails to

account for the processes occurring in hydrothermal systems, whereby the extremely low $\delta^{15}\text{N}$ values are from isotopically fractionated N_2 degassing from geothermal waters, not mixing with mantle components (see main text). Bottom, we show the values for $\text{N}_2/{}^3\text{He}$ versus $\delta^{15}\text{N}$ for air, the convective mantle and cratonic gases compared with samples from this study. This is a similar plot to that in Sano et al.³² except that cratonic gases are defined (see the Supplementary Information). The samples with low $\text{N}_2/{}^3\text{He}$ values relative to the cratonic endmember can be assumed to receive negligible cratonic nitrogen (see the main text and Supplementary Discussion on Yellowstone). The mantle gases are taken from ref.³.



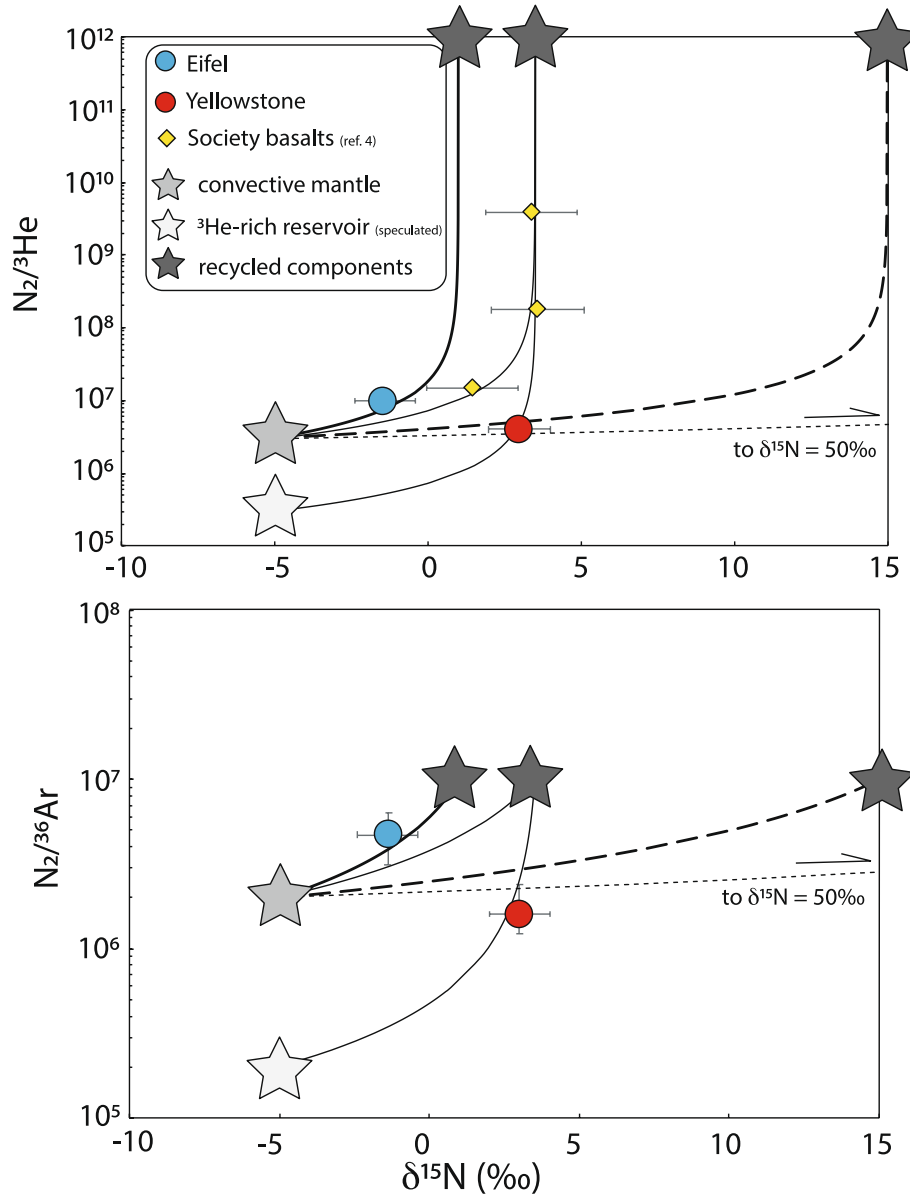
Extended Data Fig. 4 | $^{84}\text{Kr}/^{36}\text{Ar}$ and $^{132}\text{Xe}/^{36}\text{Ar}$ ratios versus $\delta^{15}\text{N}$ in gases from hydrothermal systems with near-atmospheric values. $^{84}\text{Kr}/^{36}\text{Ar}$, $^{132}\text{Xe}/^{36}\text{Ar}$ and $\delta^{15}\text{N}$ values are shown for Iceland and Yellowstone samples for which we have heavy noble gas data and Δ_{30} values of 16‰ and higher. In the two plots, the data define a negative trend, implying that nitrogen loss causing $\delta^{15}\text{N}$ variations occurs together with preferential Kr (top) and Xe (bottom) losses

relative to argon. This is in contrast with predictions based on solubilities obtained in ideal conditions, where both Kr and Xe are expected to be more soluble than Ar²⁹. We suggest that this represents degassing of air-saturated water under extreme temperature and pressure conditions, where gas solubilities deviate considerably from behaviour governed by Henry's Law²⁹. Here, the data would require Kr (and Xe) to become more insoluble than Ar.



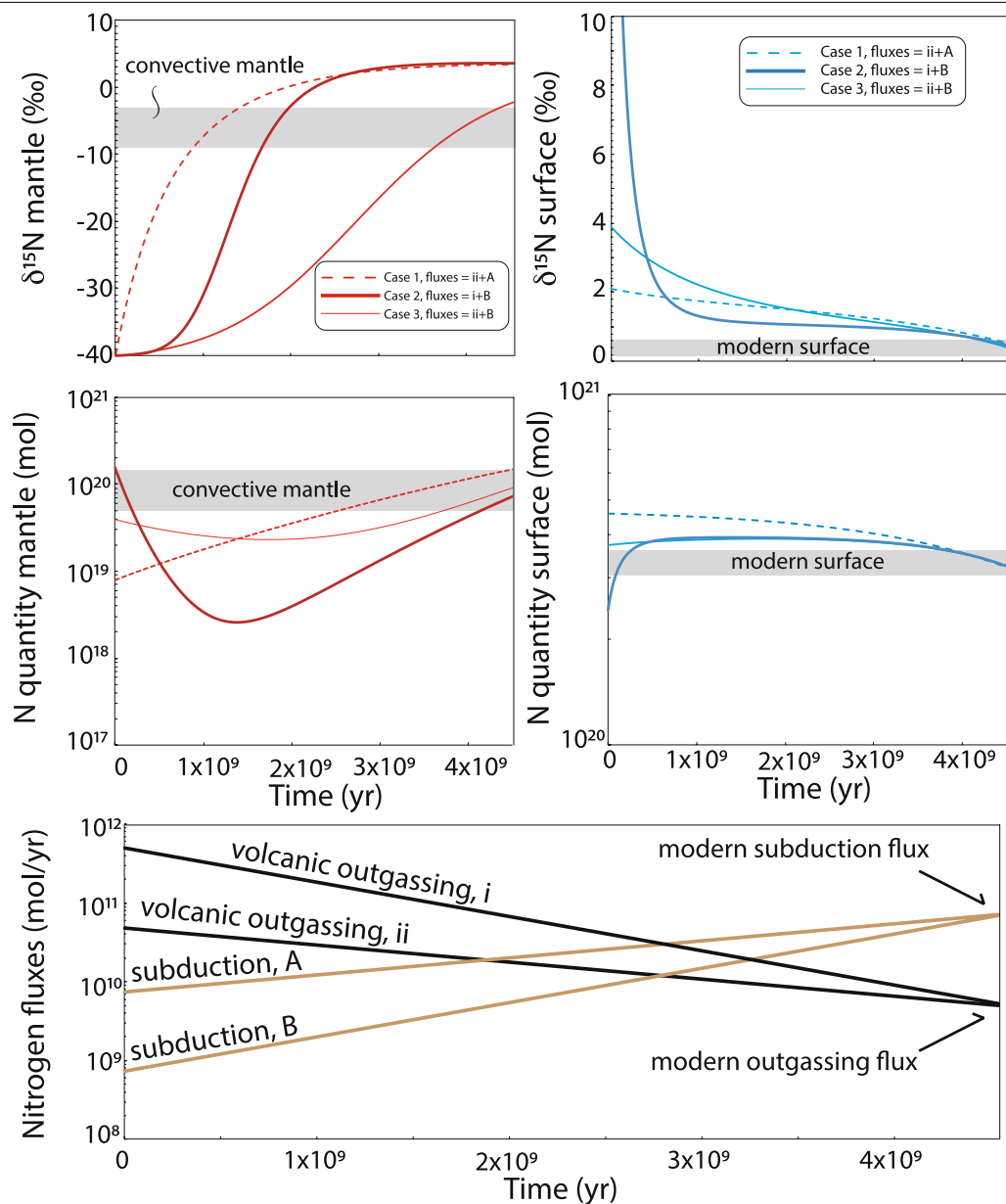
Extended Data Fig. 5 | $N_2/^{36}Ar$ ratios versus $^{40}Ar/^{36}Ar$ ratios in basalts and rocks from the Kola plume. Data are from the literature^{2-4,86} and illustrate mixing between mantle gases and air, most probably as the result of the introduction of air into rock cracks during eruption or sample handling. The highest $^{40}Ar/^{36}Ar$ ratio recorded in basalt crushing experiments with simultaneous $N_2/^{36}Ar$ measurements is $42,366 \pm 9,713$. At this value, the corresponding $N_2/^{36}Ar$ ratio is $4.2^{+2.0}_{-1.5} \times 10^6$, which was assigned to the

convective mantle⁸⁶. The convective mantle is more likely to have a $^{40}Ar/^{36}Ar$ ratio of $25,000 \pm 2,000$ (ref. ⁴⁴). At this $^{40}Ar/^{36}Ar$ ratio, the corresponding $N_2/^{36}Ar$ value becomes $2.0^{+1.0}_{-1.2} \times 10^6$. At a $^{40}Ar/^{36}Ar$ value of 5,000 (refs. ^{2,4}), the plume $N_2/^{36}Ar$ value would be lower, at $0.4^{+0.2}_{-0.2} \times 10^6$. However, at the $^{40}Ar/^{36}Ar$ value of 10,000 suggested by recent studies³¹, we obtain $N_2/^{36}Ar = 0.7^{+0.5}_{-0.3} \times 10^6$ for the plume according to the correlation between $N_2/^{36}Ar$ and $^{40}Ar/^{36}Ar$.



Extended Data Fig. 6 | Mass balance applied to account for Eifel and Yellowstone, in terms of $\delta^{15}\text{N}$, $\text{N}_2/{}^{36}\text{Ar}$ and $\text{N}_2/{}^3\text{He}$. $\delta^{15}\text{N}$ values of Eifel and Yellowstone are shown, as derived from Fig. 1. $\text{N}_2/{}^{36}\text{Ar}$ and $\text{N}_2/{}^3\text{He}$ values of Eifel and Yellowstone are also shown, as derived from Figs. 2, 3. Recycled components have high elemental ratios, according to ref. ³². These ratios might be even higher if N was less devolatilized than noble gases during slab devolatilization. Note that this would not change our conclusion, since the mixing curve would remain identical. **a**, In the $\text{N}_2/{}^3\text{He}$ space, the position of Eifel and society basalts can be explained with a simple two-component mixing between the convective mantle and some recycled component. The values for the three Society basalts are taken from ref. ⁴. The dataset was filtered to show only basalts with the lowest levels of air contamination. We only used the three

basalts with ${}^{40}\text{Ar}/{}^{36}\text{Ar} > 5,000$. For this to work for Yellowstone, anomalously high $\delta^{15}\text{N}$ would be required (see **b**). An alternative mixing requires a ${}^3\text{He}$ -rich reservoir to be postulated with a low $\text{N}_2/{}^3\text{He}$ ratio. We illustrate this speculation with a $\delta^{15}\text{N}$ of -5‰, like that of the convective mantle. However, other $\delta^{15}\text{N}$ values (typically between -10 and +10‰) would also fit the Yellowstone data. This is because N in the Yellowstone source would mostly be accounted for by the recycled component, not the ${}^3\text{He}$ -rich endmember forced with a low $\text{N}_2/{}^3\text{He}$ ratio **b**. In the $\text{N}_2/{}^{36}\text{Ar}$ space, Eifel can be explained by conventional mixing. If such mixing involves the known convective mantle, Yellowstone requires a recycled endmember with a $\delta^{15}\text{N} > 50$ ‰, which is implausible. Again, for a mixing to account for the data, one would have to assign the ${}^3\text{He}$ -rich reservoir with a low $\text{N}_2/{}^{36}\text{Ar}$ ratio.



Extended Data Fig. 7 | The evolution of $\delta^{15}\text{N}$ and nitrogen abundances in the convective mantle and at the Earth's surface as a function of time. Various cases with time-dependent solutions are explored. Curves are calculated as for Fig. 4 (main text) using a two-box model described in the Methods and main text. Here, three cases are modelled on the basis of the combination of various temporal variations in volcanic outgassing and subduction fluxes shown in the bottom panel. Modern fluxes are taken from ref.¹³. The blue curves (right) are for the surface (air + continental crust), and the red curves (left) are for the convective mantle. As in Fig. 4, the starting composition for the mantle was chosen to have an enstatite chondrite-like $\delta^{15}\text{N}$ (ref.⁶), and various initial N abundances. A critical result of the model is that varying fluxes can easily match the N abundances for the mantle and the surface, as well as the isotope

composition of N in the surface. However, similar to the case where constant fluxes are used (Fig. 4), relatively high subduction fluxes pushes the N isotope cycle towards a steady state in which the mantle would have a higher average $\delta^{15}\text{N}$ value than that of the surface, contrary to the relationship observed today. The model shown as Case 3 provides an acceptable match to the modern observations, where the mantle has a $\delta^{15}\text{N}$ value of -1‰ , after starting at -40‰ . However, this predicts that the mantle evolves considerably through time in terms of $\delta^{15}\text{N}$. Thus, if correct, this prediction requires all peridotitic diamonds to be formed in roughly the past 500 Myr. However, peridotitic diamonds found in cratonic lithospheres as old as 3.3 Gyr old are dominated by a $\delta^{15}\text{N}$ mode at -5‰ (ref.¹⁸), seemingly ruling out the Case 3 model.